EARLY APTIAN AND ALBIAN (MID-CRETACEOUS) GEOCHEMICAL AND PALYNOLOGICAL RECORDS FROM THE EROMANGA BASIN (AUSTRALIA): INDICATION OF THE TOOLEBUC FORMATION BEING AN EXPRESSION OF OAE 1C

Abstract

The GSQ Hughenden-7, GSQ Manuka-1, and GSQ Eromanga-1 cores from the Eromanga Basin were studied for palynology, organic-carbon-isotope ($\delta^{13}C_{org}$) stratigraphy and total organic carbon (TOC) content. The dinocyst events combined with the $\delta^{13}C_{org}$ records inferred an Early Aptian to Late Albian age for the studied sections. Comparison of the data with information from the Carpentaria Basin reveals that the start of the mid-Cretaceous marine incursion into the Eromanga Basin is related to the earliest Aptian sea-level rise. Further comparison with time-equivalent Tethyan records shows that the Toolebuc Formation within the three cores is linked with oceanic anoxic event (OAE) 1c in the earliest Late Albian. The Toolebuc Fm reflects three depositional modes: firstly, a sea-level rise caused leaching of nutrients and primary productivity strated to increase; secondly, a sudden short-term sea-level fall associated with the highest primary productivity observed for the Toolebuc Fm; and thirdly, a sea-level rise with increased influx of terrestrial derived material. Further palaeoenvironmental reconstructions, based on selected groups within the dinoflagellate cysts and sporomorph assemblages, indicate relatively cooler and drier conditions at the onset of the Toolebuc than for the later part when conditions become warmer and more humid.

1. Introduction

In sedimentary sections Oceanic Anoxic Events (OAEs) are generally characterized by enrichment of organic matter, lamination, the absence or strong impoverishment of benthic faunas, and rising ^{13}C / ^{12}C values of inorganic and organic carbon (Kuypers, 2001). Although these characteristics apply to almost all OAEs, the events differ significantly in detail. To explain the occurrence of these widespread anoxia two contrasting models were postulated. In the first, preservation is improved due to oxygen depletion (e.g. Schlanger and Jenkyns, 1976; De Boer, 1986). The dysoxic or anoxic conditions created at the seafloor are caused by an enhanced stratification of the water column and result in better preservation of organic matter (e.g. Bralower and Thierstein, 1984). The second model is a high productivity model (e.g. Pederson and Calvert, 1990). This model requires sufficient ventilation and nutrient recycling. Due to enhanced primary productivity more oxygen is consumed during sedimentation of the organic matter, eventually leading to a surplus in organic matter, which is stored in the sediment (e.g. Pederson and Calvert, 1990; Hochuli et al., 1999).

The Toolebuc Formation from the Eromanga Basin in Australia is characterized by an inter-layering of organic carbon-rich and calcareous material. The presence of benthic faunas throughout this formation, indicates that truely anoxic conditions did not develop during deposition of the black shale layers. According to Shafik (1985) and Bralower et al. (1993) the Toolebuc Fm correlates to the the nannofossil *Axopodorhabus albianus* Zone (NC 9B subzone) and the planktic foraminifera *Biticinella breggiensis* Zone, linking the Toolebuc Fm to OAE 1c (Bralower et al., 1993). Besides this information, little is known on the timing of the Australian Toolebuc 'event.'

To determine the driving forces behind the Toolebuc Formation and their relation with the global OAE 1c event, here the palynological, organic-carbon-isotope and total organic carbon records for three cores from the Eromanga Basin are compared to data currently assigned to OAE 1c. The three selected cores from the Eromanga Basin are the Geological Survey of Queensland (GSQ) Hughenden-7, GSQ Manuka-1, and GSQ Eromanga-1. For comparison of the data, the same palynological and geochemical methods and techniques as in the previous chapter have been applied.

2. Geological setting

During the Early Cretaceous a marine incursion invaded the Eromanga Basin, forming a shallow epeiric sea covering part of inland eastern Australia. This basin was connected with the Carpentaria Basin across the Euroka Arch to the north and with the Surat Basin across the Nebine Ridge to the southeast (Figure 1). The three basins collectively is referred to as the Great Artesian Basin, which extends over approximately 1.7 million km^2, about one-fifth of present-day Australia.
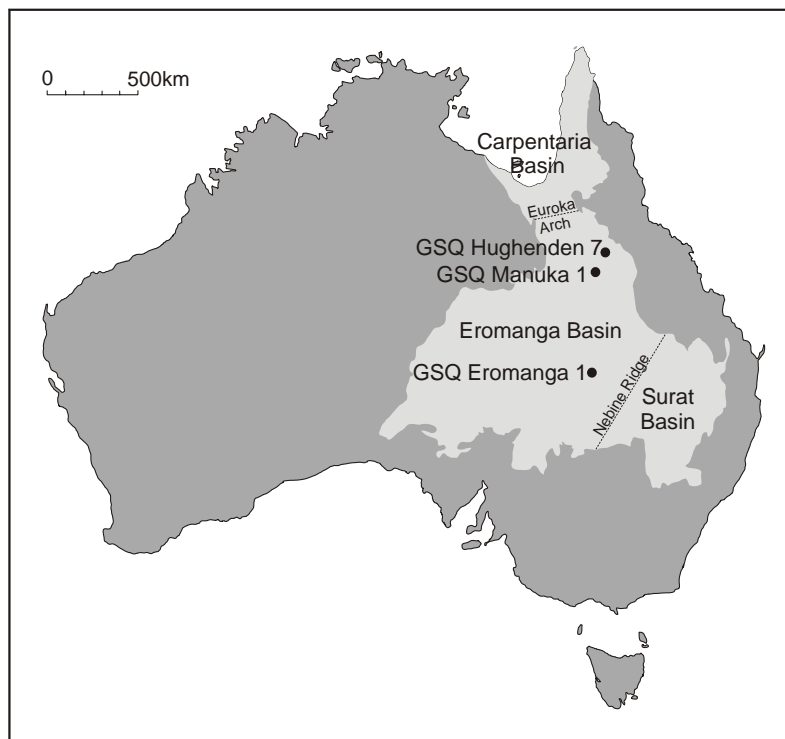

Figure 1. Map with present coastline of Australia showing locations of GSQ Hughenden-7, GSQ Manuka-1 and GSQ Eromanga-1; shaded area outlines the Cretaceous, epicontinental Carpentaria, Eromanga and Surat basins.

The formal lithostratigraphy of the Eromanga Basin was established by Vine and Day (1965) and Vine et al. (1967). Based on the lithological and biostratigraphical data by the mid seventies (e.g. Evans, 1966; Day, 1969; Dettmann and Playford, 1969; Burger, 1973a, b; Haig, 1979), the tectonic and sedimentological history of the basin was reconstructed by Exon and Senior (1976). Later Morgan (1980b) summarized in great detail the palynostratigraphic and lithostratigraphic development for the Early and Middle Cretaceous of the Australian Basins. For the Eromanga Basin he interpreted the data in terms of eustatic sea-level variations and proposed several successive transgression-regression cycles (Morgan, 1980b, figure 20; included here as Figure 2).

The oldest lithological unit sampled from the Eromanga Basin for this thesis is the Cadna-owie Formation. This formation was defined by Wopfner et al. (1970) from the Early Cretaceous of the Eromanga Basin in South Australia. Senior et al. (1975) showed that it extends eastward over much of the Eromanga Basin in Queensland. The formation has been subdivided into two units. The lower (unnamed) interval of siltstone and minor sandstone and mudstone is considered to represent a middle Neocomian transgression (cycle β in Morgan, 1980b; Figure 2) progressively resulting in deposition of fluvial, to littoral, to shallow marine sediments. The successive Wyandra Sandstone Member, comprising laminated to massive sandstones is inferred to represent beach and/or fluvial deposits as result of a regression (end of cycle β in Morgan, 1980b; Figure 2). Both units of the Cadna-owie Formation are suggested to correlate to the *Foraminisporis wonthaggiensis* sporomorph Zone (Morgan, 1980b) from the Australian Mesozoic zonation scheme (Helby et al., 1987, figure 19).

The boundary between the Cadna-owie and the stratigraphic higher Wallumbilla Formation is considered to be diachronous, and marks the transition to a major transgression (cycle γ in Morgan, 1980b; Figure 2).

The Wallumbilla Formation is a sequence of marine mudstone, siltstone and very fine labile sandstone (Vine & Day, 1965). In the northern and central parts of the Eromanga Basin the formation is subdivided into the Doncaster member, Jones Valley Member, and Ranmoor member (Vine & Day, 1965), and in the southern and eastern parts in the Doncaster and Coreena members (Morgan, 1980b; Figure 2).

In general the Doncaster Member comprises mudstone, siltstone, minor sandstone and limestone and is considered to represent shallow marine deposits (Exon and Senior, 1976). The Jones Valley Member is an interval of siltstone, calcareous siltstone, limestone, and silty, very fine sandstone (Exon and Senior, 1976), which presumably represents paralic conditions. The Ranmoor Member contains mudstone and siltstone, which are carbonaceous in part, and is considered to represent shallow marine to paralic circumstances (Exon and Senior, 1976). The lateral equivalent, the Coreena Member, consists of interlaminated and interbedded sandstone and siltstone, as well as mudstone and siltstone. Both members were supposedly deposited along the basin margin (Morgan, 1980b).

Morgan (1980b) assigned the lower Wallumbilla Formation to his *Odontochitina operculata* dinoflagellate Zone, the middle part to the *Pseudoceratium turneri* Zone; and the upper part to the basal *Endoceratium ludbrookiae* Zone. Later Helby et al. (1987) incorporated these zones into their Australian Mesozoic zonation scheme and correlated them, respectively, to uppermost Barremian-middle Aptian, middle Aptian-Upper Albian and Upper Albian-Upper Cenomanian. In addition to corresponding to a dinocyst zonal boundary the base of the Wallumbilla Formation approximates the base of the *Cyclosporis hughesii* sporomorph Zone, which presumably correlates to the Early Aptian (Helby et al., 1987; Chapter 3). Two more sporomorph zones were identified in the Wallumbilla Formation: the *Cyclosporites striatus* Zone (presumed uppermost Aptian-Lower Albian) and the *Coptospora paradoxa* Zone (presumed middle Albian) (biostratigraphic correlations after Helby et al., 1987). The Wallumbilla Formation is inferred to encompass two Aptian and two Albian transgressions (cycle γ, δ, ε and onset of ζ in Morgan, 1980b; Figure 2) and is conformably overlain by laminated mudstone of the Toolebuc Formation.

The Toolebuc comprises bitumous and calcareous shale, fossiliferous limestone and is in general easily recognized on the basis of a strong gamma-ray anomaly in wireline-logging (Exon and Senior, 1976). This unit is interpreted to have been deposited in a shallow sea with good connection to the open ocean in the north (Exon & Senior, 1976) and it is considered to represent the maximum flooding interval of a transgressional cycle (part of cycle ζ in Morgan, 1980b). This unit correlates to the lower part of the *Endoceratium ludbrookiae* dinocyst Zone (Morgan, 1980b), later retained and incorporated by Helby et al. (1987; presumed early Late Albian). The Toolebuc is conformably overlain by the Allaru Mudstone Formation which comprises highly fossiliferous
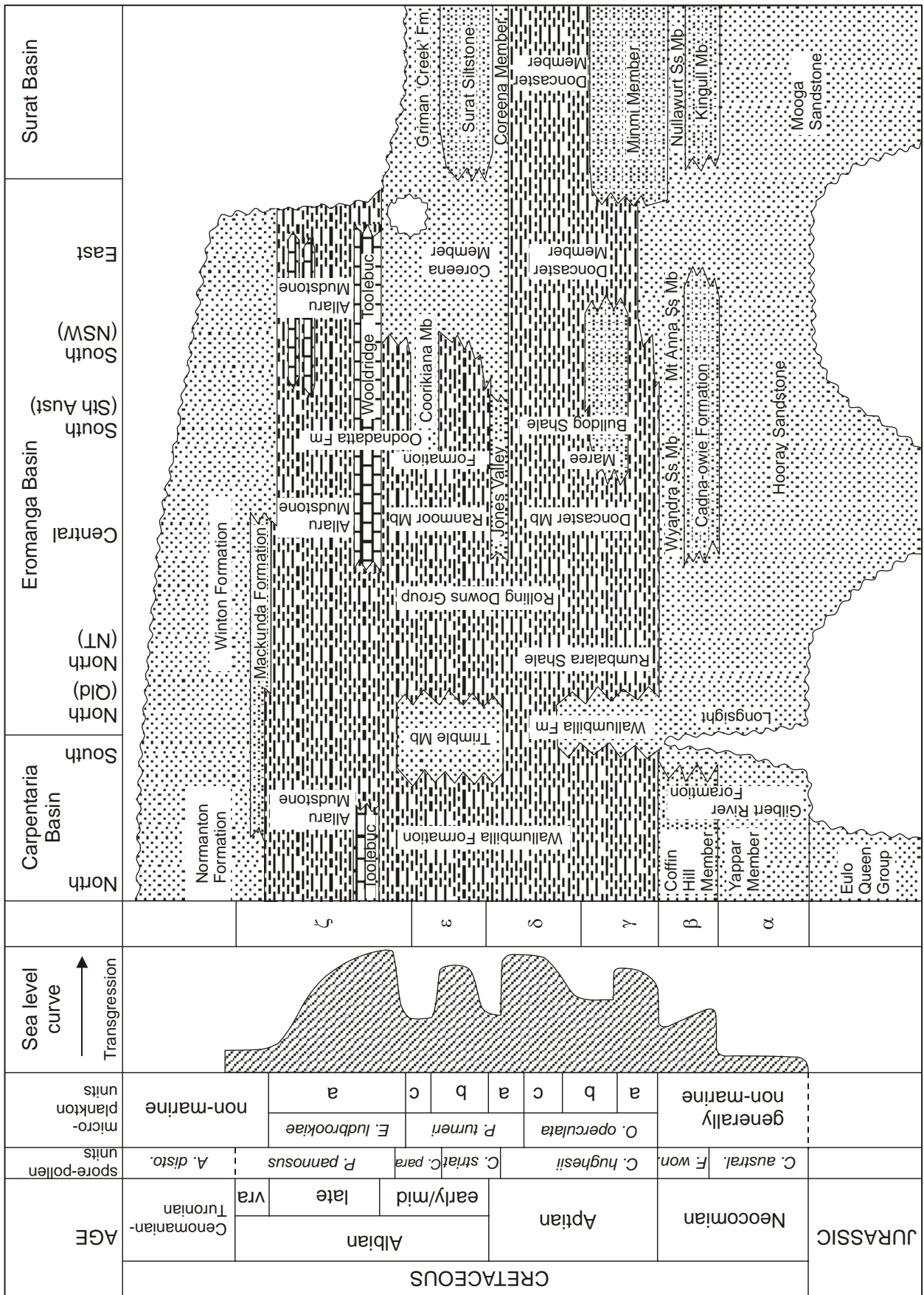
Figure 2. Summary of the geology of the Cretaceous, epicontinental basins from Morgan (1980b, figure 20). (coarse stipple = sandstone; fine stipple = siltstone; horizontal shading = mudstone; brickwork = limestone)

mudstone. In some successions the transition between the formations is hard to trace and merely based on a change in color (e.g. Almond, 1983). The Allaru Mudstone reflects a return from more open marine to shallow marine conditions (regression of cycle ζ in Morgan, 1980b). This unit correlates with the remainder of the *E. ludbrookiae* dinocyst Zone and the *Phimopollenites pannosus* sporomorph Zone (Helby et al., 1987; presumed Late Albian). In the northern Eromanga Basin this formation is succeeded by the Mackunda Formation, which predominantly consists of sandstone, siltstone, and mudstone, representing slightly marine and paralic environments (Exon and Senior, 1976; continued regression of cycle ζ in Morgan, 1980b).
Morgan (1980b) inferred that Early Cretaceous tectonic processes in and around the Eromanga Basin were simple, slow and uniform downwarping.

3. Material and Methods

The three selected cores from the Eromanga Basin (i.e., GSQ Hughenden-7, GSQ Manuka-1, and GSQ Eromanga-1) lie along a nearly north-south transect (Figure 1). These cores were drilled during the late seventies to early eighties by the Department of Mines and are currently stored at the Geological Survey of Queensland (GSQ) in Brisbane. This study focuses on the palynological and geochemical content of the cores. The palynological study involves quantitative dinocyst analysis. The geochemical study focuses on the organic-carbon-isotopes ($\delta^{13}C_{org}$), total organic carbon (TOC), and carbonate content (Carb %).

3.1 *Cores and lithology*

The cores will be discussed from the most northern to southern location, i.e., from GSQ Hughenden-7 to Manuka-1 to Eromanga-1.

3.1.1 *GSQ Hughenden-7*

In 1977 drilling the Hughenden-7 hole in the northern Eromanga Basin at 20°57′S and 144°11′E was completed (Figure 1). Approximately 895 m of presumably Lower Cretaceous to Permian rocks were recovered. The basic lithostratigraphy of the core was described in a report (Balfe, 1979; Figure 3). Of the six formations recovered at Hughenden-7 two were sampled for this study. From top to bottom these units are:
- the Toolebuc Formation (14–21 m). The formation overlies the preceding Wallumbilla Formation conformably and comprises laminated dark grey to black shale with a few laminae of clean limestone (Balfe, 1979). The black shale is strongly calcareous, in part fissile, and has a soapy texture (Balfe, 1979). The limestone is most common in the top 2 meter of the core and consists of remains of large marine bivalves (e.g., of *Inoceramus* and *Aucellina*). Fish remains are also common; especially in the intervals 16.05-16.25 m, 17.50-17.90 m, and 18.40-19.70 m. The formation shows a strong positive anomaly in gamma-ray (Balfe, 1979).
- the Wallumbilla Formation (21–177 m). Balfe (1979) differentiated several sandstone units within this formation. The most prominent ones lie between: 64 and 68 m (tentatively defined as the Jones Valley Member), 80 and 100 m (containing an interval at around 90 m with evidence of bioturbation and infilling, and planar crossbedding), and between 137 and 146 m (tentatively as the Doncaster Member). Campbell and Haig (1999) reported three further sand units, i.e.: between 110 and 111.6 m, 116 and 120.04 m, 148 and 150 m.
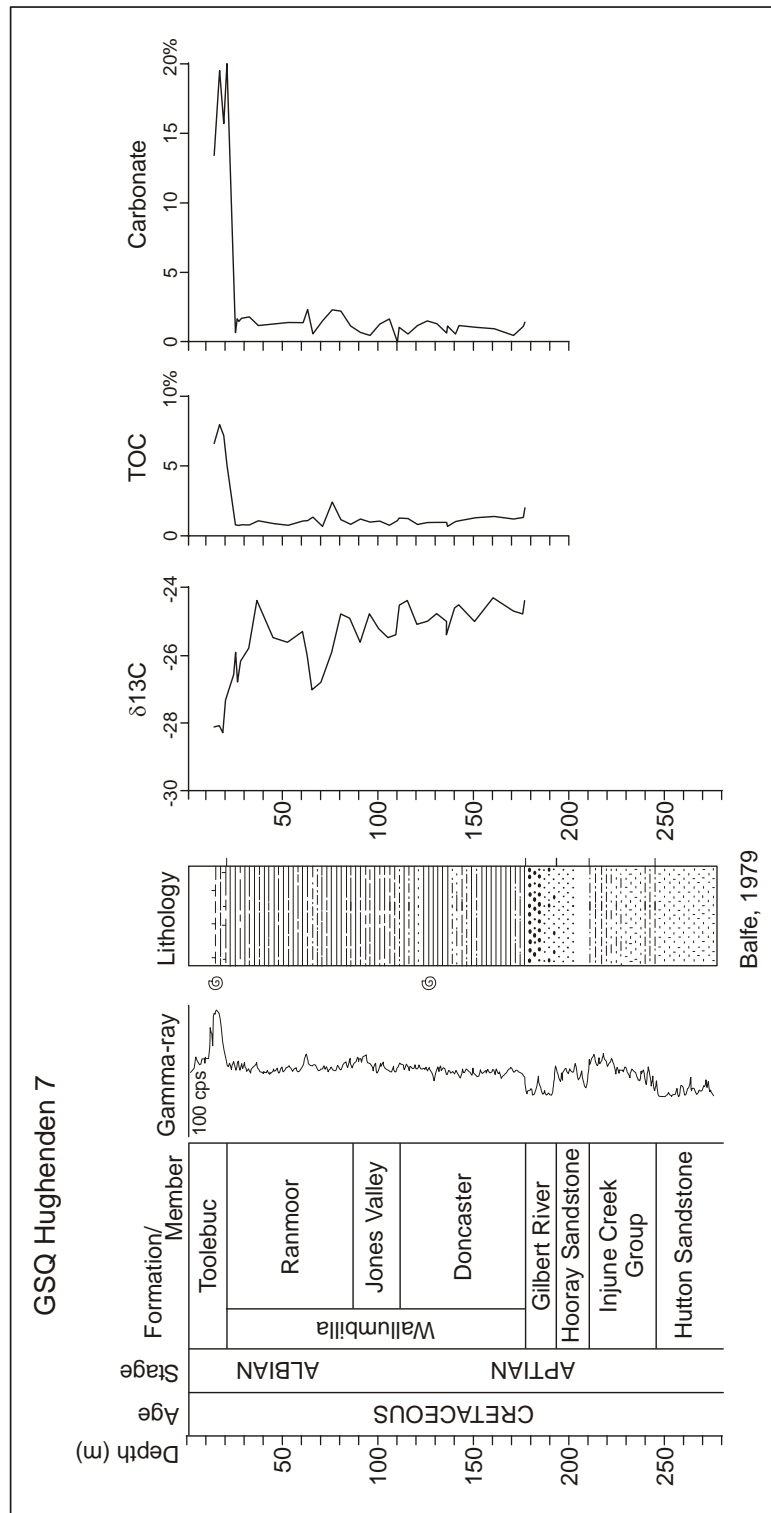
Figure 3. The stratigraphical and lithological column at GSQ Hughenden-7 (adapted from Balfe, 1979) with organic-carbon-isotope (d13Corg), total organic carbon (TOC) and carbonate content measured for the section (this study).

Based on mainly qualitative palynological data, Burger (1982) approximated the boundaries between the Ranmoor – Jones Valley members above 111.61 m and the Jones Valley – Doncaster boundary to lie around 120.04 m. On foraminifera, Haig and Lynch (1993) did not differentiate the Jones Valley Member. Consequently, the Ranmoor Member lies immediately on top of the Doncaster Member, at around 92.6 m. In Campbell and Haig (1999) however, the Jones Valley Member is questionably assigned to the sandstone interval between 64 and 68 m.

Below the Wallumbilla lies an interval comprising of sandstone and conglomorate in a coarsening up sequence, which Balfe (1979) assigned to the Gilbert River Formation, as described from the Carpentaria Basin (Liang and Power, 1959). Morgan (1980b; Figure 2) did not differentiate this formation in the Eromanga Basin.

In additional foraminiferal studies Haig and Lynch (1993) and Campbell and Haig (1999) correlated samples from: 16.63 and 19.89 m to the planktic *Hedbergella* association (zone of dwarf *Hedbergella*) of presumed late Middle Albian to earliest Late Albian; samples from the interval between 26.47 and 60.26 m partly to the benthic *Ammobaculites* association (*Eomarssonella crespinae* Zone) and the planktic *Hedbergella* association (*Hedbergella planispira* Zone) of presumed late Early Albian-early Middle Albian; the interval between 64.73-82.99 m was correlated to the benthic *Ammobacculites* association of presumed Early Albian age; the interval from 86.83-144.77 m was assigned to the *Ammobaculites* association (*Aaptotochoichus pitmani* Zone) of presumed earliest Albian age.

Burger (1982) differentiated four sporomorph zones within the Toolebuc and Wallumbilla formations in Hughenden-7. From top to bottom these zones are: *P. pannosus* (from 24.75-28.50 m, with a tentative lower boundary), *C. paradoxa* (29.35-66.00 m), *C. striatus* (77.50-111.61 m), and the *Osmundaciidites dubius* (120.04-174.40 m). These zones were later incorporated in the Helby et al. (1987) sporomorph zonation scheme for the Mesozoic of Australia in which the first three zones were maintained, but the *O. dubius* Zone was included in the *C. hughesii* Zone.

3.1.2 *GSQ Manuka-1*

In 1976 the Manuka-1 hole was drilled in the northern Eromanga Basin at 21°43′59″S and 143°22′10″E (Figure 1). The hole was to provide a cored and wireline logged reference section through the Mesozoic, and to investigate the oil shale prospects of the Toolebuc Formation. A total depth of 900.4 m was reached with almost complete core recovery between 17.0–782.3 m and 789.7 m to total depth, which contains presumed Cretaceous and Upper Jurassic sediments. The lithostratigraphy was reported by Balfe (1978) and later information on foraminifera was published (Haig, 1979; Haig and Lynch, 1993; Campbell and Haig, 1999).

Nine lithological units were recovered from Eromanga-1 (Balfe, 1978; Figure 4). Samples used in this study originate from the interval between 240.29–756.65 m, comprising part of five formations. From top to bottom the units studied are:
- lower part of the Mackunda Formation (144–244 m).
- Allaru Mudstone Formation (244–510 m).
- Toolebuc Formation (510–544 m), subdivided into an upper part (510–532) and lower part (532–544 m). The upper part consists of dark gray calcareous shale with abundant laminae of crystalline calcite comprising bivalve remains of *Inoceramus* and *Aucellina* (can constitute up to 20 to 30% of the total rock). Balfe (1978) observed few scattered fish remains within this part; between 516-519 m and 524-526 m. The lower part comprises dark, calcareous, pyritic shale with abundant fish remains (Figure 4). The fish remains are common throughout this part and can form distinct beds of up to 50 mm thick, which further contain abundant rounded glauconitic grains (0.5-1.0 mm in diameter; Balfe, 1978). Between 542 and 543 m, Balfe (1978) observed abundant ammonites, which are in common partially or completely pyritized. Pyritic nodules are common in the lower part.
- Wallumbilla Formation (544–725 m); although the subdivision into members is difficult a number of coarser intervals (of which the two thickest occur between 592-605 m and 633-637 m, might correspond to the Jones Valley Member (Balfe, 1978). Based on foraminifa, Haig and Lynch (1993, figure 15) initially placed the Jones Valley Member between 633 and 637 m, but later Campbell and Haig (1999) placed it between 592 and 605 m. In Campbell and Haig (1999)
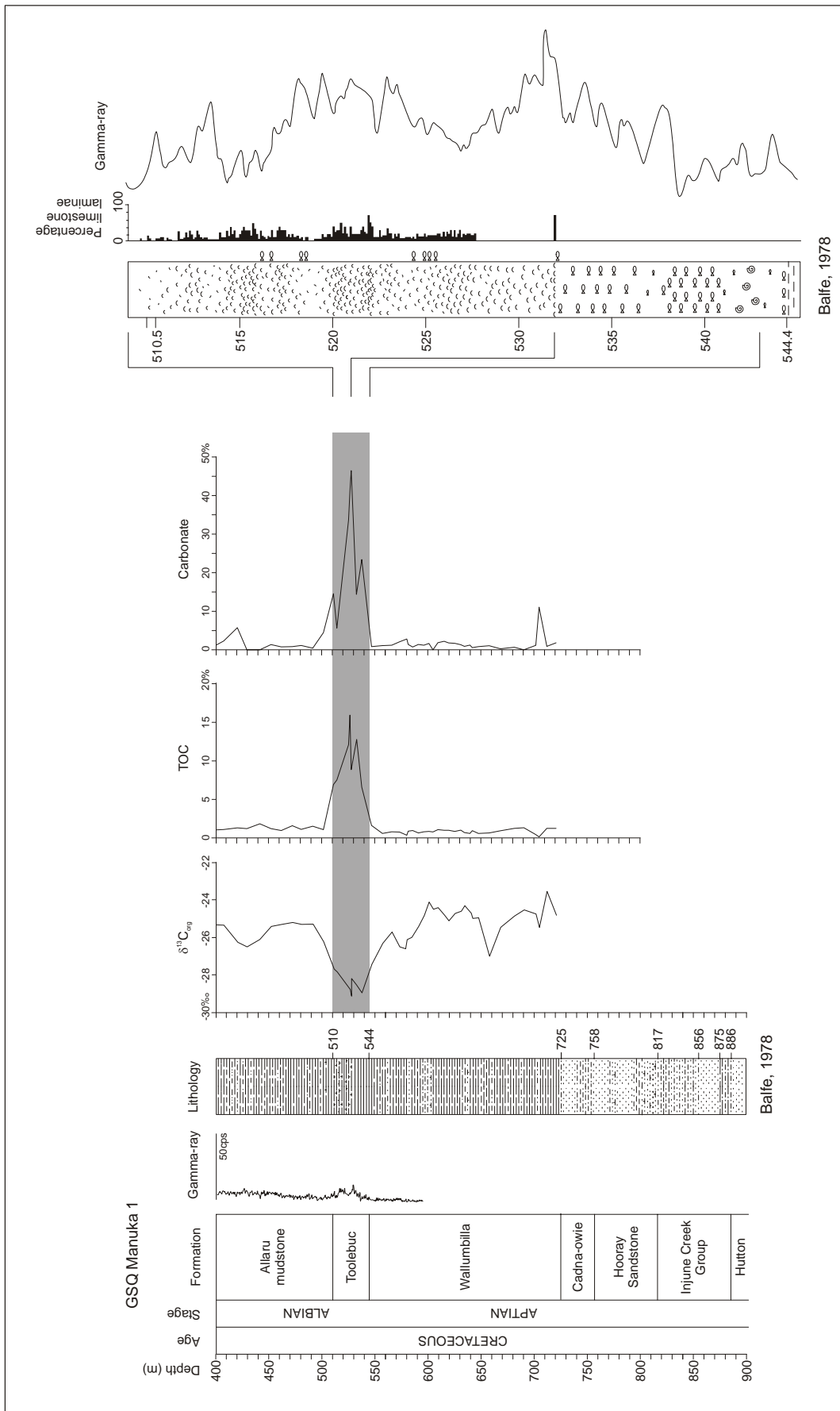
Figure 4. The stratigraphical and lithological column at GSQ Manuka-1 (adapted from Balfe, 1978) with organic carbon isotope (d13Corg), total organic carbon (TOC) and carbonate content measured for the section (this study).

the Doncaster Member correlates to the interval between 608-725 m and the Ranmoor Member to 544–598 m.

- Cadna-owie Formation (725–758 m), comprises very fine to coarse sandstone (dominant) and lesser silty shale, silty sandstone and mudstone (Balfe, 1978).

Foraminifera were studied by Haig and Lynch (1993) and Cambell and Haig (1999). These studies correlated samples from: 509.39–519.83 m to the zone of dwarf *Hedbergella*; 532.35–541.02 m to the benthic *Ammobaculites* association (*E. crespinae* Zone) overlapped by the planktic *Hedbergella* association (zone of dwarf *Hedbergella*) of presumed late Middle Albian to earliest Late Albian; the sample at 541.02 m contains the *Ammobaculites* association with dwarf representatives of the species (*E. crespinae* Zone) of presumed late Middle Albian; samples from the intervals between 549.51–591.77 m to the *Ammobaculites* association (*E. crespinae* Zone); and from 598.84 m to the *Ammobaculites* association (*A. pitmani − E. crespinae* Zone) of presumed earliest Albian age; samples from the interval 608.98–680.73 m to the *A. pitmani* Zone of presumed Late Aptian; the interval from 727–724 m contains the *Textulariopsis cushmani* Zone of ?Barremian to Early Aptian

3.1.3 *GSQ Eromanga-1*

In 1982 drilling the Eromanga-1 hole in the central Eromanga Basin at 26°36′54″S and 143°52′44″E was completed as part of a program to understand regional stratigraphy. A total of 1257.4 m of Jurassic and Cretaceous sedimentary rocks were intersected. These overlie low-grade metamorphosed sedimentary rocks of probable Palaeozoic age (Almond, 1983). Total depth was reached at 1266.9 m. The lithostratigraphy was described by Almond (1983; Figure 5). The material used in this study comes from the interval between 401.86–814.76 m and from top to bottom comprises:

- Allaru Mudstone Formation (265.8–463.7 m).
- Toolebuc Formation (463.7–473.4 m). The formation can be subdivided into two major intervals subdivided by a conglomorate. The lowermost interval (from 469.4-473.4 m) consists of dark grey mudstone, which is: slightly silty; poorly sorted; poorly laminated; contains sparse, small pelecypods; and common shell fragments. Toward the top of this lower interval the mudstone grades into laminated, fissile siltstone and silty fine to very fine-grained sandstone overlain by 20 mm of buff sandy siltstone (Almond, 1983). This lower interval is overlain by 30 mm of conglomorate, which consists of clasts of very fine-grained sandstone and siltstone in a muddy calcareous matrix, and which correlates to a gamma-ray anomaly. The upper interval (from 463.7-469.4 m) consists of laminated and subfissile, dark grey mudstone, which contains some fish scales and ammonites and pelecypods replaced by pyrite. Upward this interval grades into the lithologically very similar Allaru Mudstone Formation. Therefore Almond (1983), selected the Toolebuc-Allaru boundary on the basis of a subtle colour change, which coincides with a decrease in the number of pelecypods replaced by pyrite (Almond, 1983).
- Wallumbilla Formation, which is further subdivided into the Coreena Member, (473.4–543.6 m) and the Doncaster Member (543.6–714.2 m).
- the Cadna-owie Formation (714.2–814.6 m), which is subdivided in the Wyandra Sandstone Member (714.2–773.7 m) and a lower unnamed interval (773.7–814.6 m; Almond, 1983).

Burger (1989) studied the lower section of the core up to 819.11 m, within the Hooray Sandstone Formation, which he inferred to correspond to his *Cicatricosisporites australiensis* Zone. Beside his study no additional information for Eromanga-1 has been published.
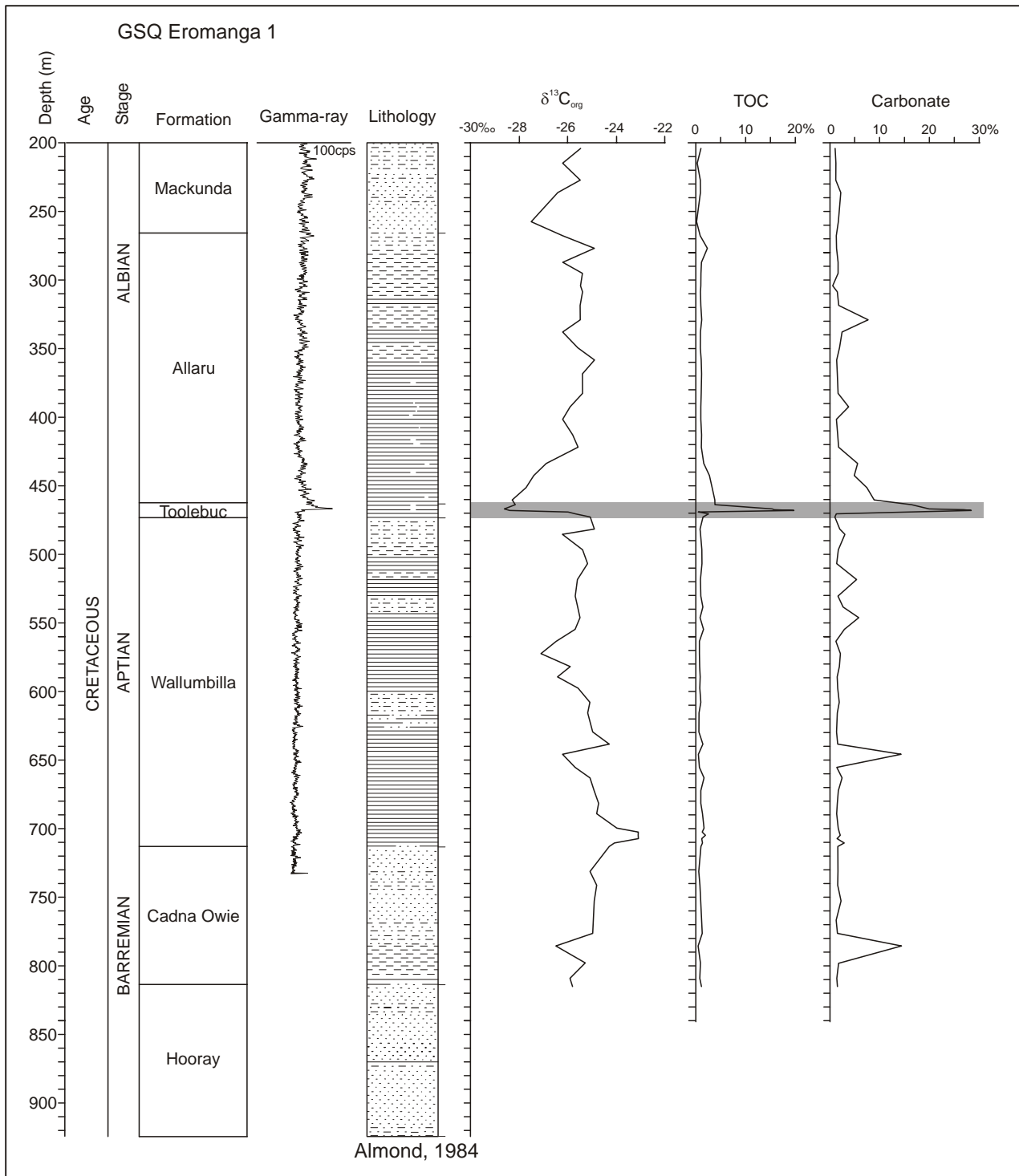
Figure 5. The stratigraphical and lithological column at GSQ Eromanga-1 (adapted from Almond, 1983) with organic carbon isotope (d13Corg), total organic carbon (TOC) and carbonate content measured for the section (this study).

3.2 *Samples*

A total of 148 samples were taken for geochemical and 106 for palynological analyses. For Hughenden-7 samples come from the interval between 21–177 m, of these 38 samples were used for geochemical and 37 for palynological analysis. For Manuka-1, between 240.29–756.65 m, 58

samples for geochemical and 38 for palynological analysis. For Eromanga-1, from 401.86–814.76 m, 52 samples for geochemical and 31 for palynological analysis.

3.3 *Palynology*

The applied methods for palynology, biostratigraphic correlation and palaeoenvironmental reconstructions are described in the corresponding section for the BMR Mossman-1 borehole from the Carpentaria Basin in Chapter 3. The quantitative distribution pattern of the palaeo-environmental dinocyst groups is shown in Figures 6, 7, 9 (variables 1 to 7) and sporomorph groups in Figures 6, 8, 10 (variable 8; see Chapter 3); the curves represent percentages of the total assemblage.

In BMR Mossman-1 the FOs of *Tehamadinium tenuiceras*, *O. operculata*, and *Carpodinium granulatum*, and the LOs of *Valensiella magna*, *Muderongia australis*, and *Epitricysta vinckensis* are accompanied by a maximum abundance of cool-temperate dinocysts and high frequencies of the heterotrophic cyst *Palaeoperidinium cretaceum*. These events in Mossman-1 correspond with organic-carbon-isotope segments C4 to C6 (Menegatti et al., 1998; Bralower et al., 1999), and to the lower *O. operculata* dinocyst Zone (earliest Aptian) in Australia. In Mossman this particular interval represents the most rapid phase of the profound transgression of the earliest Aptian Ap3 stratigraphical sequence of Jacquin et al. (1998). The consequential maximum flooding in Mossman-1 is reached in an interval with maximum $\delta^{13}C_{org}$ values of isotope segment C7, and sea level inferred to fall in isotope segment C8 (Mossman-1, Chapter 3), with sequence boundary Ap4 of Jacquin et al. (1998) represented in its upper part.

The upper *O. operculata* Zone is indicated by the first appearances of *Diconodinium* spp and *Spinidinium boydii* (Helby et al., 1987). This zone is succeeded by the *Diconodinium davidii* Zone, and the boundary between the two is defined by the FO of *Endoceratium turneri* (Helby et al., 1987). However, in the Eromanga Basin, the inception of *E. turneri* may lie higher within the *D. davidii* (Morgan 1980a). Morgan (1980b) inferred a major regression within the *D. davidii* Zone (his *P. turneri* subzone a), below which level *D. cerviculum* and *M. tetracantha* are common, and above which level dinocysts in general become less common.

The *D. davidii* zone corresponds to isotope segments C9 and C10 and contains the sequence boundary Ap5 of Jacquin et al. (1998).

The LO of *D. davidii* defines the base of the succeeding *Muderongia tetracantha* Zone. According to Helby et al. (1987) *Litosphaeridium arundum* incepts at the base of the *M. tetracantha* Zone. In Europe the FO of *L. arundum* is reported from the lowermost Tethyan *tardefurcata* ammonite Chronozone and in the Boreal *mammilatum* ammonite Chronozone: as such the inception approximates the Aptian-Albian boundary (Leereveld, 1995; Hart et al., 1996). Immediately below the Stage boundary lies Ap6, marking the onset of a next rapid phase of the earliest Albian transgression (Hardenbol et al., 1998; Jacquin et al., 1998).

Based on foraminiferal and nannofossil data Bralower et al. (1999) inferred the Aptian-Albian boundary to lie at the base of carbon isotope segment C11. This implies that the base of the *M. tetracantha* Zone would correlate with C11, which would then confirm the assessment by Helby et al. (1987).

The LO of *M. tetracantha* marks the base of the following *Canninginopsis denticulata* Zone. The base of the stratigraphic younger *Endoceratium ludbrookiae* Zone is defined by the FO of *E. ludbrookiae* (Helby et al., 1987).

The Toolebuc Formation and its lateral equivalents in the Eromanga Basin fall within the lower *E. ludbrookiae* Zone (McMinn and Burger, 1986). Bralower et al. (1993) determined the Toolebuc Formation to contain the early Late Albian NC 9B nannofossil zone, which correlates to OAE 1c. Consequently, this zone corresponds with global isotope segments C14 (showing a profound drop in $\delta^{13}C_{org}$), and C15 (the return to more positive $\delta^{13}C$ values; see Bralower et al., 1999). According

to Erbacher et al. (1996) the organic rich shales related to OAE 1c mark the inflection point of a major regression in sea level.

3.4 *Geochemistry*

Carbon isotope measurements were carried out on the organic carbon fraction of samples, with TOC analyses made on the same samples. For isotope analysis samples of shale were crushed to powder in a Tima mill, then treated with 10% HCL for carbonate removal, followed by rinsing in distilled water and freeze drying. Sample aliquots were combusted in a Carlo Erba NCS 1500 element analyzer. After purification, the gas products were chromatically separated, and subsequently analyzed by a Prism III Micromass Stable Isotope Mass Spectrometer at the University of Wollongong. Contents were determined by standard comparison using paired urea and sucrose standards. Precision of the analyses for replicate samples and standards is better than 0.3‰. Data is reported in standard delta notation ($\delta^{13}C$) relative to Pee Dee belemnite.

The $\delta^{13}C_{org}$ records for the Eromanga cores have been approached the same way as BMR Mossman-1, for which is referred to the corresponding section in Chapter 3.

4. Results

4.1 *Palynology*

In general, the samples contain abundant sporomorphs and dinocysts; acritarchs and acid-resistant foraminiferal linings are mostly rare. There is a wide range in the state of preservation: assemblages from mud- and siltstones are well-preserved and relatively rich, while those from sandier intervals are generally poorer. Diversity in the palynological assemblages within the three Eromanga cores varies from extremely low to high. The quantitative dinocyst distribution charts for Hughenden-7, Manuka-1 and Eromanga-1 is given in Tables 7, 9 and 11, respectively, and the quantitative spore-pollen data in Tables 8 (Hugheden-7), 10 (Manuka-1) and 12 (Eromanga-1).

The palynological assemblages from the Cadna-owie Formation contain high numbers in sporomorphs and hardly any dinocysts. Within the Wallumbilla Formation sporomorphs dominate the sandier intervals while dinocysts dominate in the shale- and mudstones; diversity is lowest in the sandier intervals. In general the Toolebuc Formation is characterized by extremely low diversity. Dinocyst diversity shows a slight increase again in the lower Allaru Formation but does not reach the level as prior to the Toolebuc Formation. Going upward in the Allaru Formation, the number of dinocysts and diversity declines in favour of the number of sporomorphs. In the upper part of this formation the number of dinocysts becomes too small to establish a statistically reliable quantitative analysis (less than 200 specimen were encountered), in this case the samples where studied qualitative for dinocysts only. The same accounts for the Mackunda Formation.

In general, peaks in diversity correspond to increased values in the cool-temperate dinocyst groups. The highest values in cool-temperate taxa are reached in the lower part of the studied intervals in the three wells.

Stratigraphically important dinocyst taxa occur in low numbers. The distribution of these key taxa is recorded in terms of first occurrence (FO) and last occurrence (LO).

When the FOs and LOs for the three cores are compared mutually and to other sequences in Australia (e.g. Helby et al, 1987; Stover and Helby, 1987a, b; Helby and McMinn, 1992; Oosting et al., in prep.; Chapter 2 and 3) seventeen diagnostic dinocyst events for pan-Australian correlations can be recognized. Combined, these comprise five, possibly six, Australian dinocyst zones (Helby et al., 1987). The composite diagnostic dinocyst events and the inferred dinocyst zones in ascending order are (Figure 6, 7 and 9):

Odontochitina operculata Zone:
1) First consistent occurrence of *O. operculata*; marks the base of the *O. operculata* Zone.
2) LO of *E. vinckensis*; lowermost *O. operculata* Zone
3) LO of *M. australis*; lowermost *O. operculata* Zone.
4) FO of *S. boydii*; lower *O. operculata* Zone.
5) LO of *Systematophora areolata*; middle *O. operculata* Zone.
6) FOs of *Diconodinium* spp and *Diconodinium pusillum*; in the middle *O. operculata* Zone.
7) LO of *V. magna*; top of the *O. operculata* Zone.
8) FO of *D. davidii*; base of the *D. davidii* Interval Zone (see comments in next section).

Diconodinium davidii Zone:
9) FO of *E. turneri*; marks the base of the *D. davidii* Zone. Although in Helby et al. (1987, figure 26) the inception of *D. davidii* is considered to be coeval with that of *E. turneri*, in the Great Artesian Basin it may occur prior to *E. turneri* (see Morgan, 1980a).
10) Acme of *D. davidii* lies within the zone.

Muderongia tetracantha Zone:
11) LO of *D. davidii*; marks the base of the succeeding *M. tetracantha* Zone.
12) FO of *L. arundum*; base of the *M. tetracantha* Zone.
13) LO of *Dingodinium cerviculum*; middle *M. tetracantha* Zone.

Canninginopsis denticulata Zone:
14) LO of *M. tetracantha*; marks the base of the succeeding *C. denticulata* Zone.
15) FO of *C. denticulata*; middle *C. denticulata* Zone.

Endoceratium ludbrookiae Zone:
16) FO of *E. ludbrookiae*; marks the base of the *E. ludbrookiae* Zone.
17) FO of *Ascodinium parvum*; middle *E. ludrookiae* Zone.

In GSQ Eromanga-1 the *Muderongia australis* Zone is tentatively identified at the base of the studied interval.

Comparison of the composite dinocyst events encountered in the Eromanga cores with ammonite calibrated formations from the Tethyan and Boreal realms (Hoedemaeker and Leereveld, 1995; Wilpshaar, 1995; Leereveld, 1997; Hoedemaeker, 1999) reveals five successive events which appear to be useful for global correlation. The three events are:
1) FO of *Odontochitina operculata*. In the Tethyan Realm it lies in the lower *vandenheckii* ammonite Chronozone (lowermost Upper Barremian; Wilpshaar, 1995). In Boreal successions its FO lies in the *elegans* ammonite Chronozone (basal Upper Barremian; Duxbury, 1980). According to Helby et al. (1987) the FO of *O. operculata* in the Austral Realm can be observed coeval with regional dinocyst events (e.g., FO of *Heerendenia postprojecta*, FO of *Ovoidinium cinctum* and FO of *Dapsilidinium ambiguum*) and in relation to global events is inferred to lie within the Upper Barremian (Oosting et al., in prep.; see Chapters 2 and 3).
2) FO of *Tehamadinium tenuiceras*. The FO of the species lies in the *tuarkyricus* ammonite Chronozone (lowest Aptian ammonite zone; Hoedemaeker and Rawson, 2000). In the Boreal realm it lies in the middle Lower Aptian *deshayesi* ammonite Chronozone (Duxbury, 1983).
3) FO of *Carpodinium granulatum*. In the Boreal realm the stratigraphic distribution is recorded to have two separate ranges of consistent occurrences (e.g. Heilmann-Clausen and Thomson, 1995). As such it does not appear a useful global marker. Its ultimate inception corresponds to the Boreal *germanica* belemnite Zone (Heilmann-Clausen and Thomson, 1995), and the Boreal *pingue/innexum* ammonite Chronozone (Mutterlose, 1992; middle Upper Barremian). If, however, in Australia its inception is related to the cooling of surface waters at the time of global carbon isotope segment C4 to C6 (Menegatti et al., 1998; see
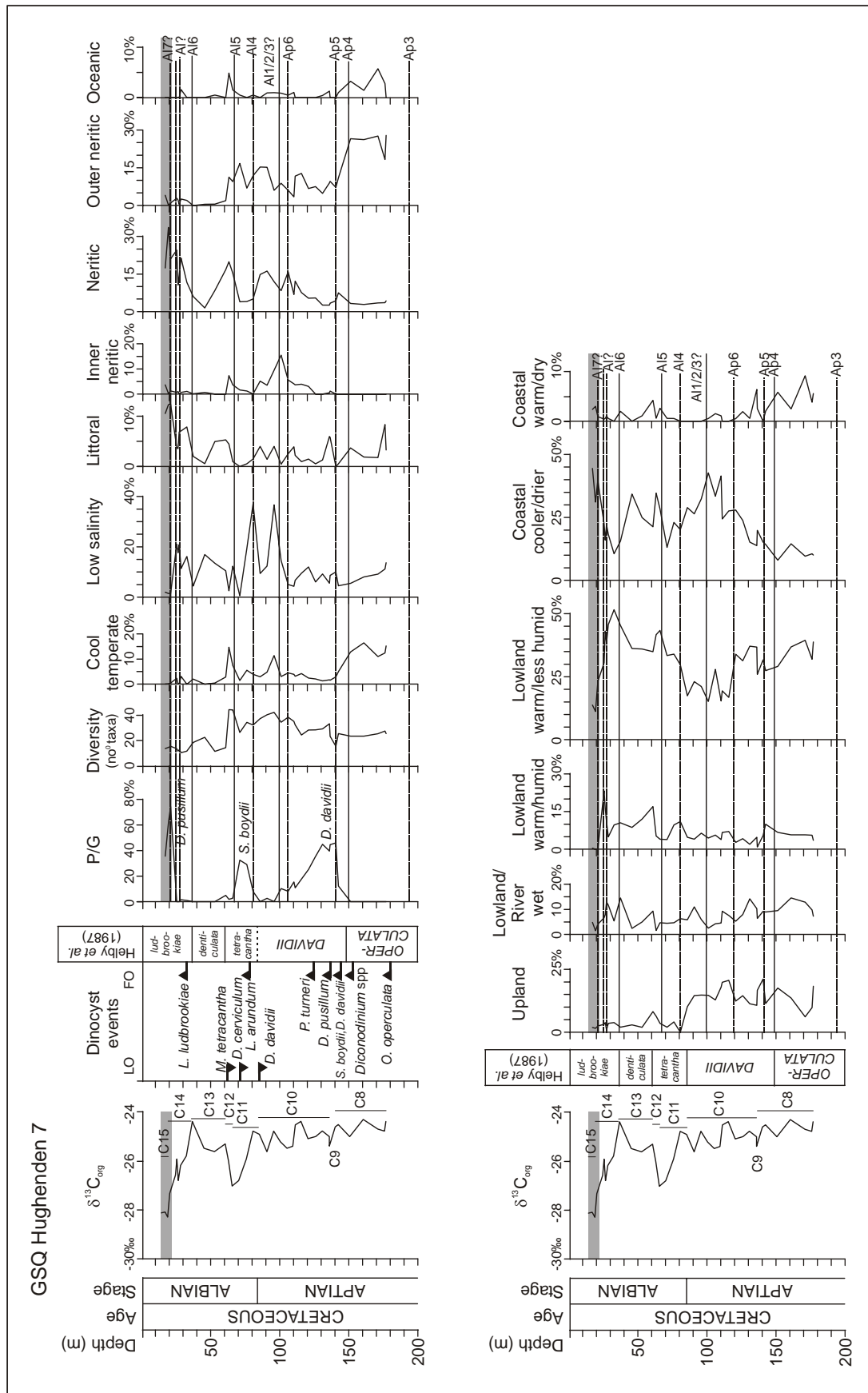
Figure 6. The GSQ Hughenden-7 carbon isotope record, dinocyst events and distribution (in percentage of total assemblage) in environmental dinocyst groups (top diagram) and patterns in environmental sporomorph groups (bottom diagram). C8 to C15 correspond to isotope segments; Ap3-Al7 on the right hand side correspond to sequence boundaries

Chapter 3), it probably coincides with the rapidest phase of the earliest Aptian transgression immediately following sequence boundary Ap3 of Jacquin et al. (1998) (see Chapter 3).

4) LO of *Valensiella magna*. The LO of this species in the Tethyan Realm is reported from the uppermost *sarasini* ammonite Chronozone (uppermost Barremian; Oosting et al., in prep.; Chapter 2). In the Boreal Realm its LO is in an interval corresponding to the middle of the *O. germanica* belemnite Zone (middle Upper Barremian; Prössl, 1990; H. Leereveld, unpublished). In the Austral Realm the stratigraphic range of the broad variety of *Valensiella* species reaches younger stratigraphic intevals (i.e., into the *O. operculata* Zone: Helby et al. (1987), i.e. Lower Aptian rather than Upper Barremian.

5) FO of *Litosphaerium arundum*. This event occurs in the lowermost Tethyan *tardefurcata* ammonite Chronozone and in the Boreal *mammilatum* ammonite Chronozone. The inception of this taxon approximates the Aptian-Albian boundary (Leereveld, 1995; Hart et al., 1996). In the Australian dinocyst zonation scheme this event lies at the base of the *M. tetracantha* Zone (Helby et al., 1987).

Images of all key dinocyst taxa are shown in Plates 7 to 14.

4.1.1 *GSQ Hughenden-7*

Palynostratigraphy

The diagnostic stratigraphical events in Hughenden-7 are comparable with the data reported by Burger (1982) and comprise five of the dinocyst zones defined by Helby et al. (1987). The zones and the diagnostic dinocyst events are:

O. operculata Zone (177.21–151.18 m), based on:
1) Presence of *O. operculata* in the lowest studied sample (177.21 m).
2) FO of *Diconodinium* spp at 151.18 m.

D. davidii Zone (151.18–86.10 m), based on:
3) FO and onset acme of *D. davidii* at 142.65 m.
4) FO of *S. boydii* at 142.65 m.
5) FO of *D. pusillum* at 136.20 m.
6) FO of *E. turneri* at 126.00 m.

M. tetracantha Zone (86.10–60.90 m), based on:
7) LO of *D. davidii* at 86.10 m. Although, its LO lies at 91.00 m in this study, Burger (1982) reported its LO from 86.10 m, in between the samples 91.00 and 86.00 m studied here.
8) FO of *L. arundum* at 76.00 m. This taxon incepts at the base of the *M. tetracantha* Zone (Helby et al., 1987, figure 26). Burger (1982) reported this species from a slightly deeper level at 77.50 m, in between the samples at 76.00 and 81.00 m used in this study.
9) LO of *D. cerviculum* at 71.00 m.
10) LO of *M. tetracantha* at 66.00 m.

C. denticulata Zone (60.90–37.29 m), based on:
Falls between LO of *M. tetracantha* and FO of *E. ludbrookiae*.

E. ludbrookiae Zone (37.29 m - top studied interval) based on:
11) FO of *E. ludbrookiae* at 20.80 m.

Palaeoenvironmental analysis

For the palaeoenvironmental reconstruction at site BMR Mossman-1 (see Chapter 3) the global carbon isotope segments were considered to reflect consecutive steps in the stratigraphic development of the basin. Recognition of these isotope segments in the basal parts of the cores from the Eromanga Basin is unfortunately not as explicit as for BMR Mossman-1 and an

alternative approach has to be used. Given that dinocysts enable a more detailed differentiation of the palaeoenvironmental development within a basin than sporomorphs, the successive dinocyst zones of Helby et al. (1987) are here taken as consecutive steps.

The quantitative distribution patterns of the selection of palaeoenvironmentally significant dinocyst groups are depicted in Figure 6. General trends in the separate intervals are discussed below.

In the *O. operculata* Zone the outer neritic group dominates while the oceanic group is also well-represented. The sudden presence of these groups is most likely linked to the rapid sea-level rise in the earliest Aptian, which quickly inundated the Eromanga Basin and led to a marine depositional environment. Towards the *D. davidii* Zone, both these groups decrease and at the base of this zone, a peak in the amount of heterotrophic species (P-G ratio), represented by *D. davidii*, can be observed. The inner neritic group culminates in the middle of the zone accompanied by a gradual increase of the neritic group. This is followed by an interval of high numbers of the low salinity group toward the top of the zone, with a corresponding slight decrease in the outer neritic group again.

The *M. tetracantha* Zone is characterized by a peak in the P-G ratio (*S. boydii*) and the outer neritic being the dominant group. The low salinity and oceanic groups show successive peaks in the top half of the zone. In the succeeding *C. denticulata* Zone the oceanic, outer and inner neritic groups are virtually absent while the low salinity group reaches high values. The neritic and littoral groups show a decrease and successive increase within the zone. In the lower part of the following *E. ludbrookiae* Zone the two latter groups together with the low salinity group are most abundant. The base of the Toolebuc Formation, which falls within this zone, is characterized by a peak in heterotrophic dinocyst types (*D. pusillum*); the littoral group reaches highest values at the top of the Toolebuc Formation.

For the quantitative distribution patterns of the palaeoenvironmental sporomorph groups the same subdivision into dinocyst zones was applied and is depicted in Figure 6.

In general the lowland, warm/temperate and less humid and the coastal cooler/relatively dry groups alternately dominate the sporomorph assemblages. From the lower part of the *O. operculata* toward the middle *D. davidii* zones, the lowland warm/temperate and less humid, the lowland/river, and the coastal warm/temperate groups show fluctuating but progressively decreasing values. The coastal cool/temperate and relatively dry group on the other hand increases. The top part of the *D. davidii* Zone is characterized by the reversed pattern, with exception of the coastal warm/temperate group which is not present. Throughout the *O. operculata* and *D. davidii* zones the upland group is well represented, contrary to the three succeeding dinocyst zones where this group only occurs in low numbers. The lowland warm/temperate and humid group shows higher values in the *O. operculata* than in the *D. davidii* Zone but for both intervals values are relatively constant.

In the *M. tetracantha* Zone the lowland warm/temperate and less humid group increase continuously and dominates the sporomorph assemblages. The coastal cool/temperate group also shows an increase, which is accompanied by the coastal warm/temperate group being present again.

The most obvious change from the *M. tetracantha* to the *C. denticulata* Zone lies in the higher values of the lowland warm/temperate and humid group and an even further decrease of the upland group. At the boundary between the *C. denticulata* and *E. ludbrookiae* zones the lowland warm/temperate less humid group reaches its maximum for the studied interval. From this point upward the three lowland groups strongly decrease while the coastal groups show an increase.

4.1.2 *GSQ Manuka-1*

Palynostratigraphy
        The FOs and LOs from Manuka-1 comprise five of the Helby et al. (1987) dinocyst zones. These and the diagnostic dinocysts in ascending order are:
O. operculata Zone (741.11–658.07 m), based on:
    1) FO of *O. operculata* at 720.33 m.
    2) FO of *Diconodinium* spp at 668.52 m.
D. davidii Zone (658.07–600.00 m), based on:
    3) FO of *S. boydii* at 658.07 m.
    4) FO and onset acme of *D. davidii* at 658.07 m.
    5) FO of *E. turneri* at 620.00 m.
    6) LO of *D. davidii* at 600.00 m.
M. tetracantha Zone (600.00–556.48 m), based on:
    7) LO of *M. tetracantha* at 556.48 m.
    8) FO of *L. arundum* at 566.14 m.
    9) LO of *D. cerviculum* at 566.14 m.
C. denticulata Zone (556.48–546.00 m).
E. ludbrookiae Zone (546.00 – top of studied interval):
    10) FO of *E. ludbrookiae* at 537.52 m.
    With middle *E. ludbrookiae* Zone:
    11) FO of *A. parvum* at 490.40m.

One further event not incorporated in the Helby et al. (1987) scheme but considered of importance is:
    12) FO of *C. granulatum* at 711.34m, within the lower *O. operculata* Zone.

The samples below 741.11 m lack dinocysts. Therefore, a dinocyst zone could not be assigned to this interval, i.e., it could already be part of the *O. operculata* Zone or correlate to the preceding *M. australis* Zone.

Palaeoenvironmental analysis
        The quantitative distribution patterns of the selection of palaeoenvironmentally significant dinocyst groups are depicted in Figure 7. Above 470 m core depth the palynological assemblages contain too little dinocysts for a quantitative analysis, those sample were omitted in the palaeoenvironmental assessment.
In broad lines the distribution patterns show similar variations within the inferred dinocyst zones for Manuka-1 as for Hughenden-7, although values for the outer neritic and oceanic groups generally reach higher values in Manuka-1. Further deviations in the patterns from Manuka are most obvious in the curve for the P-G ratio (i.e., the peak in *D. davidii* does not occur immediately at but just above the zonal boundary and reaches higher values (>70%), contrary to *S. boydii* which abundance only shows a minor increase in the *M. tetracantha* Zone, and the abundance of *D. pussilum* in the *E. ludbrookiae* Zone almost reaches 100%) and the low salinity group, which reaches a maximum in the *M. tetracantha* Zone instead of in the *D. davidii* Zone.

The sporomorph distribution patterns are shown in Figure 8. The lowland warm/temperate and less humid group dominates the assemblages while the coastal cool/temperate group forms an important constituent as well. The overall patterns are not as pronounced as in Hughenden-7 and some of the general characteristics differ as well, i.e. the lowland/river group reaches slightly higher values in the *D. davidii* than in the *O. operculata* Zone. The lowland warm/temperate and humid group fluctuates around 7% in the *O. operculata* and *D. davidii* zones; and around 3% in
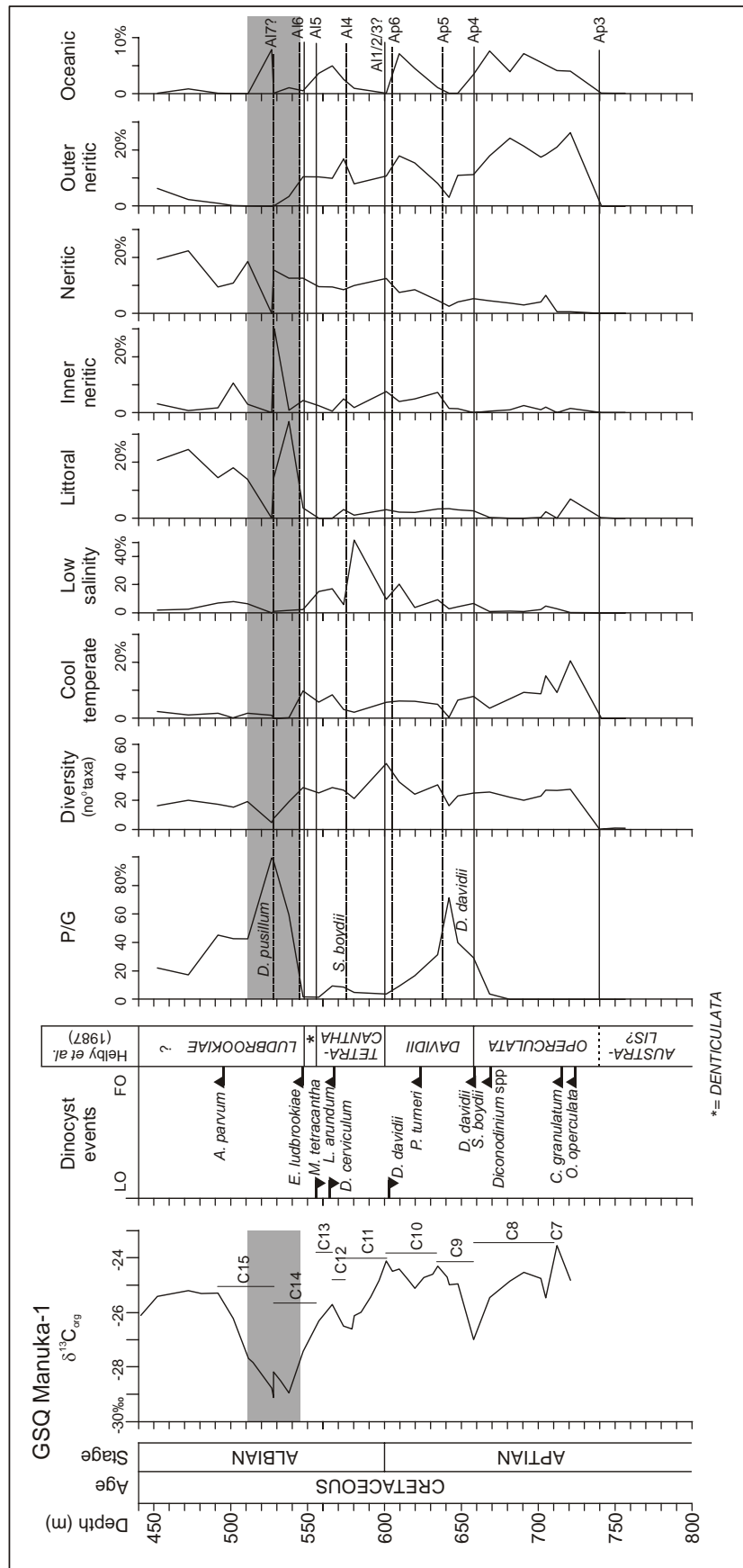
Figure 7. The GSQ Manuka-1 carbon isotope record, dinocyst events and distribution in environmental dinocyst groups (in percentage of total assemblage). C7 to C15 correspond to isotope segments; Ap3-Al7 on the right hand side correspond to sequence boundaries.
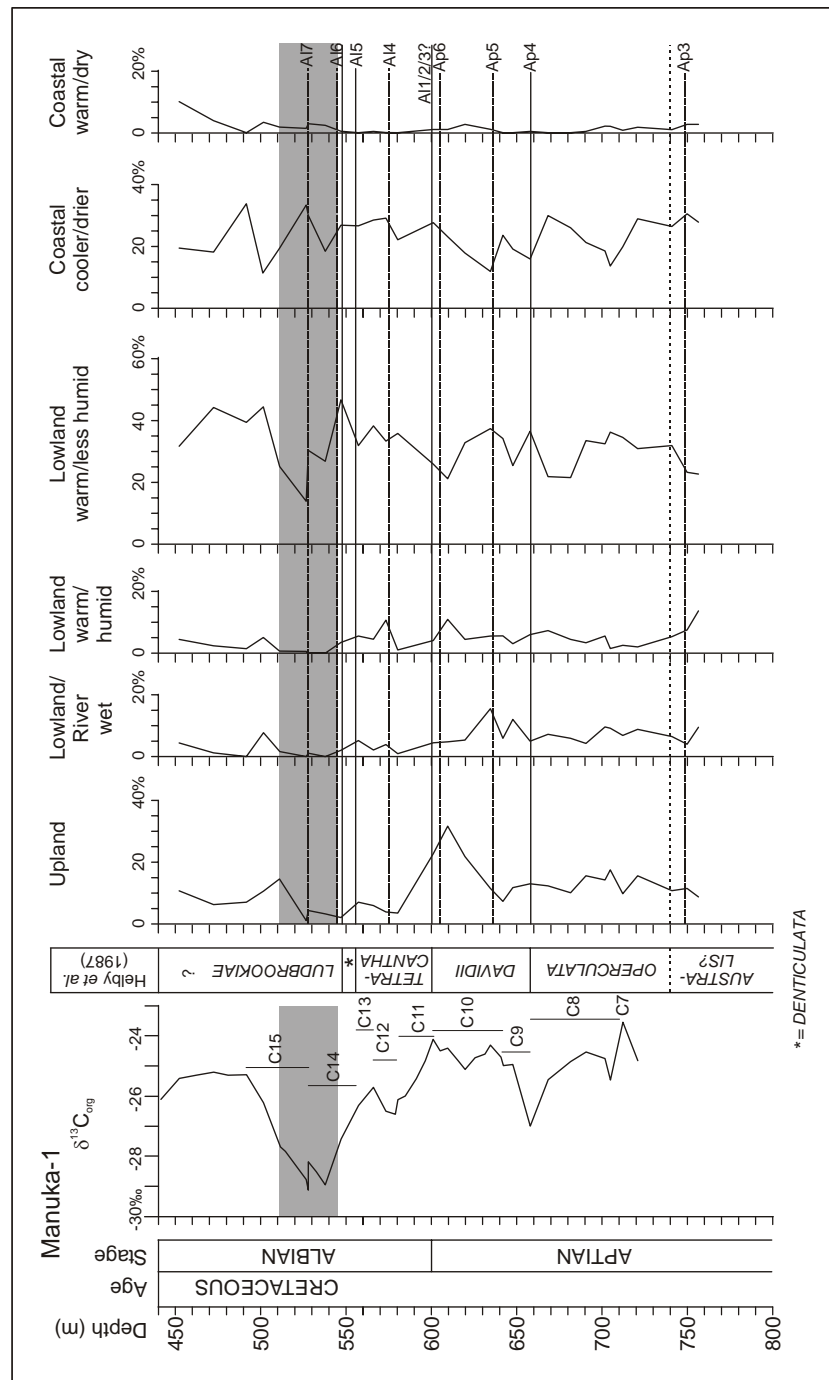
Figure 8. The GSQ Manuka-1 carbon isotope record and distribution in environmental sporomorph groups (in percentage of total assemblage). C7 to C15 correspond to isotope segments; Ap3-Al7 on the right hand side correspond to sequence boundaries.

the *M. tetracantha*, *C. denticulata*, and *E. ludbrookiae* zones, in contrast to Hughenden-7 where the opposite is the case. For the Toolebuc Formation within the *E. ludbrookiae* Zone, the patterns from the two cores are the same: after the Toolebuc, the lowland warm/temperate and less humid group reestablishes itself and becomes the dominant group again. With exception at 327 m core depth it remains the largest group.

4.1.3 *GSQ Eromanga-1*

Palynostratigraphy

The FOs and LOs observed for Eromanga-1 comprise six, with one tentative, dinocyst zones defined by Helby et al. (1987) and in ascending order these and the diagnostic events are:

?*M. australis* Zone: (below 715.83 m):

Prior to the FO of *O. operculata*; see number 15 at the end of this section

O. operculata Zone (715.83–663.87 m), based on:

1) LO of *V. magna* at 715.83 m.
2) FO of *O. operculata* at 715.83 m.
3) LO of *S. areolata* at 715.83 m.
4) LO of *M. australis* at 715.83 m.
5) LO of *E. vinckensis* at 715.83 m.

D. davidii Zone (663.87–608.22m), based on:

6) FO of *S. boydii* at 663.87 m.
7) FO of *D. davidii* at 663.87 m.
8) LO of *D. davidii* at 608.22 m.
9) FO of *Endoceratium* spp at 608.22 m; this FO is based on an operculum of an *Endoceratium* but identification to species level is not possible; the FO of *E. turneri* lies at 572.75 m.

M. tetracantha Zone (608.22–530.67 m), based on:

10) LO of *D. cerviculum* at 581.68 m.
11) FO of *L. arundum* at 563.40 m.
12) LO of *M. tetracantha* at 530.67 m.

C. denticulata Zone (530.67–482.11 m). Determining the zonal boundary between the *C. denticulata* − *E. ludbrookiae* for Eromanga-1 is also based on isotopic and lithostratigraphic signatures and elaborated on later.

E. ludbrookiae Zone (482.11 m – top of the studied interval), based on:

13) FO of *E. ludbrookiae* at 443.25 m.
14) FO of *C. denticulata* at 443.25 m.

Four additional events from Eromanga-1, which are not incorporated in the Helby et al. (1987) zonation scheme, but considered of importance:

15) LO of *Fusiformacysta salisii* at 785.00 m. In Morgan (1980a) *F. salisii* shows a LO at the top of an unnamed unit of undifferentiated Neocomian age, which proceeds his *O. operculata* subzone A, corresponding to the *O. operculata* Zone of Helby et al. (1987). Indicating that this part may corresponds to either the fluviatile equivalent of the *O. operculata* Zone or to the upper part of the *M. australis* Zone of Helby et al. (1987).
16) FO of *T. tenuiceras* at 715.83 m, within the lower *O. operculata* Zone, in the earliest Aptian (see BMR Mossman-1, Chapter 3).
17) FO of *C. granulatum* at 710.38 m, within the lower *O. operculata* Zone.
18) FO of *Psaligonyaulax deflandrei* at 460.73 m. According to Morgan (1980a) this taxon incepts at the top of his *Endoceratium turneri* subzone C, which is almost equivalent to the *C. denticulata* Zone of Helby et al. (1987).

Palaeoenvironmental analysis

The quantitative distribution patterns of the palaeoenvironmental dinocyst groups are depicted in Figure 9. Samples at 401.86 m, from the interval between 482.11–507.55 m, and below 730 m core depth contain insufficient dinocysts for a quantitative analysis, these intervals are indicated by dotted lines. The *M. australis* Zone is tentatively assigned to the interval below 725 m. At the transition to the *O. operculata* Zone all groups appear. At the base of this zone *P.*

108

cretaceum shows a peak in the P-G ratio and successively the inner neritic and neritic, outer neritic, and oceanic groups show a peak in abundance. The following *D. davidii* Zone is characterized by a peak in the eponymous species. At the base of this zone the oceanic group is most abundant but is replaced by the inner neritic and neritic groups towards the top. The succeeding *M. tetracantha* and *E. ludbrookiae* zones recognized in Eromanga-1 show the same overall changes within the distribution patterns as for Hughenden-7 and Manuka-1. The *C. denticulata* contains the interval (from 482.11-507.55 m) with very few dinocysts.

The sporomorph distribution patterns are shown in Figure 10. The patterns in general are comparable to those from Hughenden-7 and Manuka-1. Here the lowland warm/temperate and less humid group dominates the assemblages, except in the Toolebuc Formation within the *E. ludbrookiae* Zone where all but the coastal cool/temperate group show a decrease in values. Otherwise all groups are present throughout.

4.2 *Geochemistry*

The data on $\delta^{13}C_{org}$ isotopes, the total organic carbon and carbonate content are given in Tables 13, 14, and 15 for Hugheden-7, Manuka-1 and Eromanga-1, respectively.

Organic-carbon-isotopes
    The stratigraphic assessments from dinocyst correlations in this study enable comparison of the $\delta^{13}C_{org}$ curve for Hughenden-7, Manuka-1, and Eromanga-1 with the curve from BMR Mossman-1 (Chapter 3) and the global Aptian and Albian records from Menegatti et al. (1998) and Bralower et al. (1999).
The global isotope segments recognized in the cores from the Eromanga Basin are segments C7 to C15 (Figures 6, 7, 9, 11). C4 to C6 were tentatively assigned based on dinocyst distribution and events and is discussed later.
The lower *O. operculata* Zone correlates to isotope segment C7, the highest $\delta^{13}C_{org}$ values reached in the studied intervals from Manuka-1 and Eromanga-1 (Figures 6 and 8). Segment C8 falls within the remainder of this zone plus the lower *D. davidii* Zone (Figures 4, 5, and 7) and is characterized by a prolonged decrease in the $\delta^{13}C_{org}$ values. Segment C9, which shows increasing values, lies in the lower to middle *D. davidii* Zone, succeeded by C10 (fluctuating but relatively level values), which ranges to the top of this dinocyst zone. Segment C11 (strong decrease) correlates to the *M. tetracantha* Zone. Segment C12 (strong increase again) in Manuka-1 and Eromanga-1 also correlates to the *M. tetracantha* Zone but in Hughenden-7 this segment corresponds to the base of the succeeding *C. denticulata* Zone. Assignment of segment C13 is also not straightforward because it can correlate to one zone (e.g., in Hughenden-7 it corresponds to the *C. denticulata* Zone only) or two (in Manuka-1 and Eromanga-1 it correlates to the upper part of the *M. tetracantha* Zone and the whole of the *C. denticulata* Zone). Segment C14 lies at the base of the *E. ludbrookiae* Zone, followed by segment C15, which lies within this zone.

Total organic carbon content
    Most striking in the TOC records for the three cores is the level values prior to and after the Toolebuc Formation, which itself is marked by extreme high TOC values; in Hughenden-7 up to 8%, in Manuka-1 15.9%, and in Eromanga-1 19.6%. Besides these excursions only a minor peak of 2.2% in Hughenden-7 can be observed in the Wallumbilla Formation but otherwise the records for the three cores remain relatively flat.
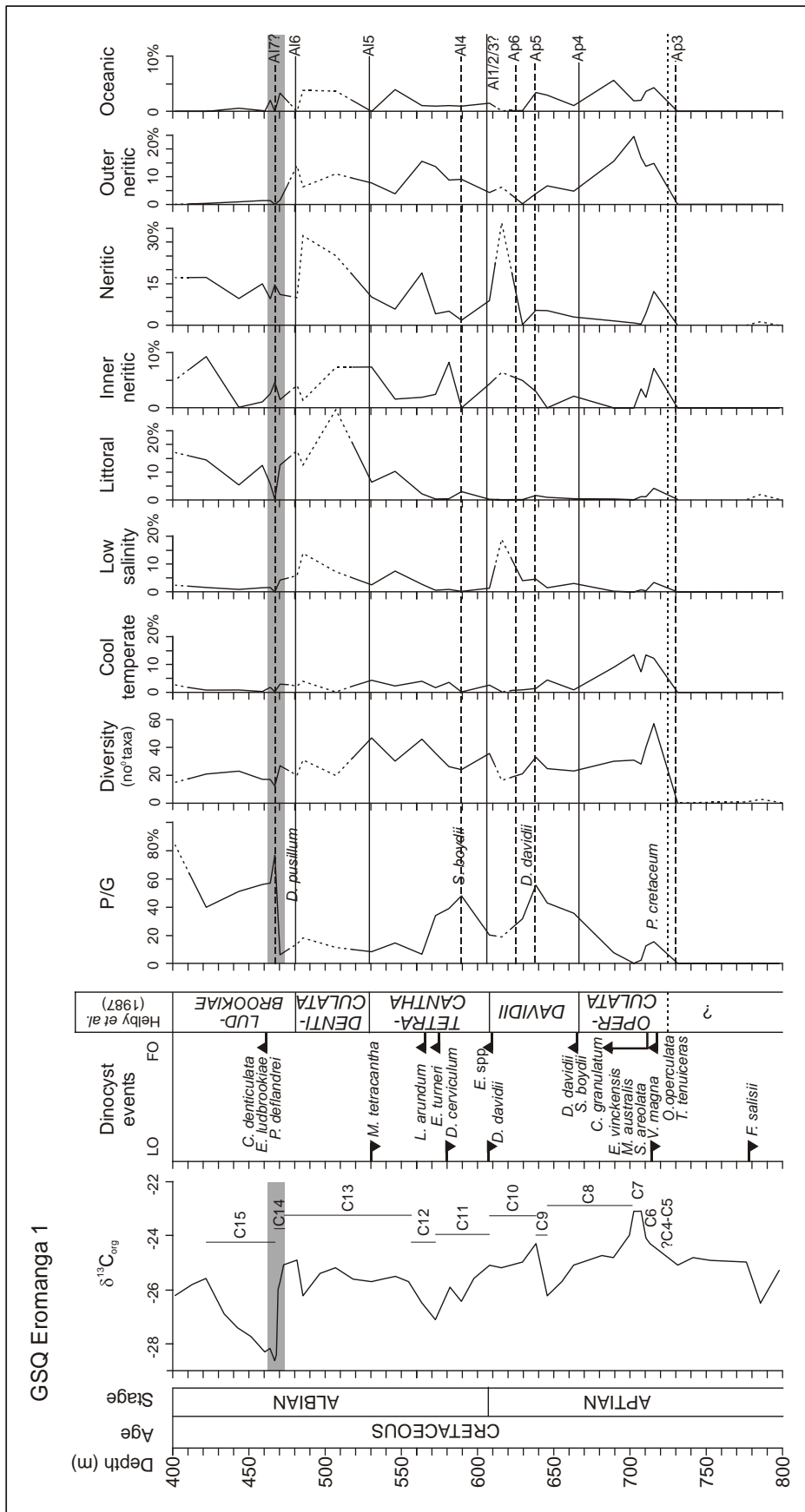
Figure 9. The GSQ Eromanga-1 carbon isotope record, dinocyst events and distribution in environmental dinocyst groups (in percentage of total assemblage). C4 to C15 correspond to isotope segments; Ap3-Al7 on the right hand side correspond to sequence boundaries.

110
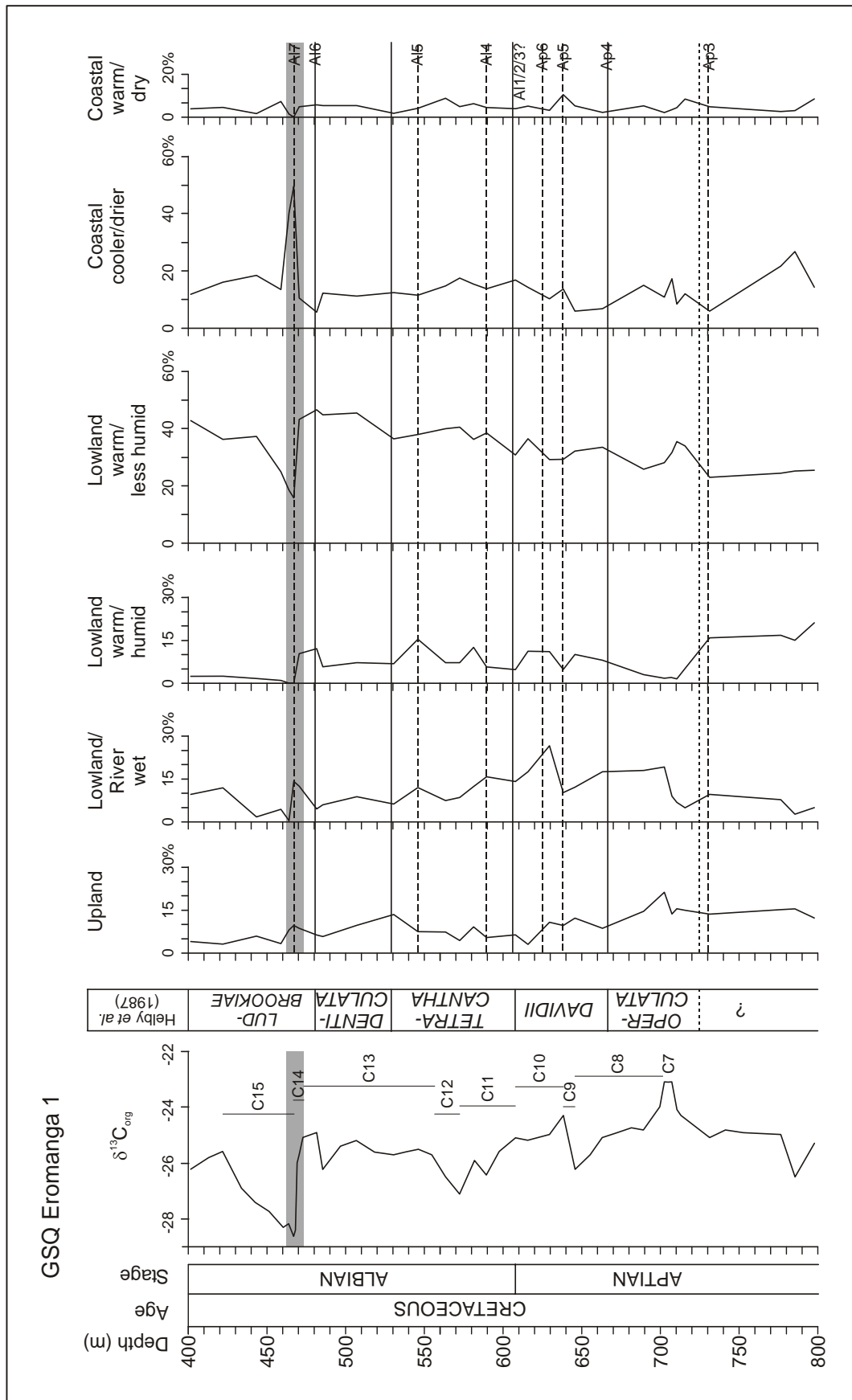
Figure 10. The GSQ Eromanga-1 carbon isotope record, and distribution in environmental sporomorph groups (in percentage of total assemblage). C4 to C15 correspond to isotope segments; Ap3-Al7 on the right hand side correspond to sequence boundaries.

Carbonate content

The CaCO$_3$% shows peak values for the three cores in relation to the Toolebuc Formation; in Hughenden-7 20%, in Manuka-1 46.4%, and in Eromanga-1 28.4%. These peaks coincide with the maximum value in TOC content.

In Eromanga-1 two further but minor peaks of 14.33% and 14.31% can be observed, in the lower Cadna-owie and in the lower Wallumbilla formations respectively. In Manuka-1, a minor peak of 11% in the lower Wallumbilla Formation is discernable; samples for the Cadna-owie Formation were not available.

5. Interpretation and integration of results

5.1 *Age assessment*

In combination with the stratigraphical organic-carbon-isotope information, the dinocyst distribution patterns in the three Eromanga cores correlate to the Early Aptian to early Late Albian. This correlation reveals that Eromanga-1 contains the stratigraphic oldest dinocysts encountered in the studied intervals. Namely, the interval from 715.83-710.38 m in Eromanga-1 contains *T. tenuiceras* and *O. operculata*, and the LOs of *V. magna*, *M. australis*, and *E. vinckensis* at 715 m and the FO of *C. granulatum* at 710.38 m. This is accompanied by high frequencies of the heterotrophic cyst *P. cretaceum*, and a maximum abundance of cool-temperate dinocysts. This sequence of events corresponds to that in BMR Mossman-1 from the Carpentaria Basin (Chapter 3) where these coincide with isotope segments C4 to C6, at the base of the Australian *O. operculata* Zone (earliest Aptian). Recognition of the isotope segments C4 to C6 in Eromanga-1 is not as straightforward as for Mossman-1, because the most distinctive characteristics cannot be observed, e.g., the negative excursion of segment C3 immediately preceding the sharp increasing values characteristic of C4, and the relatively constant values of segment C5. In Mossman this particular interval represents the most rapid phase of the profound transgression of the earliest Aptian Ap3 stratigraphical sequence of Jacquin et al. (1998). Because in Eromanga-1 samples below 715.83 m do not contain marine dinocysts the marine incursion into the Eromanga Basin probably started at the onset of the most rapid phase of the Ap3 transgression (earliest Aptian; see Chapter 3, Figure 9). This approximation is supported by the maximum in $\delta^{13}C_{org}$ values characteristic for isotope segment C7, which is reached immediately above this level.

In Manuka-1 and in Hughenden-7 this full succession of events cannot be observed but these cores do show a maximum abundance in cool-temperate dinocyst taxa in the lowest interval with marine dinocysts. In Manuka-1 the successive FOs of *O. operculata* and *C. granulatum* occur at 720.33 and 711.34 m respectively, and correlates with the highest δ^{13}C isotope values observed for this core, probably representing isotope segment C7. This level is therefore inferred to correspond to the level just above the peak in *P. cretaceum* in Eromanga-1. In Hughenden-7 a maximum in the carbon isotopes is not present but the occurrence of *O. operculata* and the high abundance of cool-temperate dinocysts in the lowest studied samples probably indicate that it correlates to the interval just above isotope segment C7 in Eromanga-1 and Manuka-1.

In the dinocyst stratigraphy from Australia the zonal boundary between the *O. operculata* and *D. davidii* zones is marked by the FO of *E. turneri* (Helby et al., 1987). In the three cores from the Eromanga Basin however, the inception of *E. turneri* lies within the latter zone (see also Morgan, 1980a) and above an acme of *D. davidii*. The FOs of *E. turneri* for the three cores studied here are therefore considered delayed and the boundary between the zones is put at the first high frequency of *D. davidii* instead, above which level *D. cerviculum* and *M. tetracantha* show a decrease (see Table 7, 9, 11).

In Hughenden-7 the FO of *L. arundum* approximates the *D. davidii* - *M. tetracantha* zonal boundary (Helby et al., 1987) but in Eromanga-1 and Manuka-1 this event lies above the base of

the *M. tetracantha* Zone. In Europe the FO of *L. arundum* is reported from the lowermost Tethyan *tardefurcata* ammonite Chronozone and in the Boreal *mammilatum* ammonite Chronozone. The inception of this taxon is thought to be the best dinostratigraphical approximation for the Aptian-Albian boundary (Leereveld, 1995; Hart et al., 1996).

In the carbon isotope records by Bralower et al (1999), the Aptian-Albian boundary lies at the base of isotope segment C11. In the cores from the Eromanga Basin the $\delta^{13}C$ values show a significant decrease and a successive increase in the *M. tetracantha* Zone, which corresponds to the pattern in the global isotope records during segments C11 and C12. This could imply that the Aptian-Albian boundary correlates with the base of the *M. tetracantha* Zone, as suggested by Helby et al. (1987).

For the cores studied here within the next stratigraphic higher *C. denticulata* Zone, no diagnostic dinocyst events were observed, and in Eromanga-1 two events frequently reported to occur within this zone have these in the succeeding *E. ludbrookiae* Zone. These events are: the FO of *C. denticulata*, in the middle *C. denticulata* Zone, and the FO of *P. deflandrei*, which is reputedly recorded to incept at the top of the *Endoceratium turneri* subzone C of Morgan (1980a), being nearly equivalent to the *C. denticulata* Zone of Helby et al. (1987).

The stratigraphic younger *E. ludbrookiae* Zone encompasses the Toolebuc Formation (McMinn and Burger, 1986). This is the case in Hughenden-7 and Manuka-1, but when applying the zonal definition at Eromanga-1, the Toolebuc would fall prior to the *E. ludbrookiae* Zone. The FO of *E. ludbrookiae* in Eromanga-1 is therefore considered slightly delayed.

The Toolebuc Formation correlates to the global isotope segments C14 (characterized by a profound drop in $\delta^{13}C_{org}$ values) and C15 (return to more positive $\delta^{13}C$ values). In Bralower et al. (1999) isotope segments C14 and C15 are inferred to correlate to early Late Albian foraminifera and nannofossil assemblages.

For the cores studied here the highest level correlates to the middle *E. ludbrookiae* Zone of the Australian zonation scheme, marked by the FO of *A. parvum*.

Because latest Albian markers were not encountered in the studied intervals from Hughenden-7, Manuka-1, and Eromanga-1, they are inferred to represent earliest Aptian to possibly early Late Albian deposits.

5.2 Reconstruction of palaeoenvironmental changes for the Eromanga Basin

Interpretation of the dinocyst records

Following the successive abundance peaks in the palaeoenvironmental dinocyst groups (Figures 4, 5, and 7), the basal parts of the Hughenden-7, Manuka-1, and Eromanga-1 cores are interpreted to represent fluviatile, relatively warm temperate conditions. This interval might correlate to the *M. australis* Zone, but to date a positive assignment is impossible because of lack of marker species from this interval in the cores.

At the base of the *O. operculata* Zone, just prior to the earliest Aptian isotope segment C7, a profound sea-level rise caused conditions to change rapidly from fluviatile to outer neritic. This rapid transgression is accompanied by a strong influence of oligotrophic waters and a high influx of cool-temperate waters (from 177.21 m in Hughenden-7, 715.83 m in Manuka-1, and 720.33 m in Eromanga-1). At this time the deepest palaeoenvironmental conditions were located around Hughenden-7.

Successively, from the base of the *D. davidii* Zone conditions change from outer neritic with oligotrophic influence toward inner neritic to neritic conditions at the top with a diminishing influx of cool-temperate waters. This relative fall in sea level is most strongly in Eromanga-1 and Hughenden-7, and least in Manuka-1, which might indicate that the center of the basin was located around the Manuka area. This sea-level drop is associated with a rapid increase in the heterotrophic *D. davidii*. The interval characterized by the *D. davidii* acme is succeeded by the *M.*

tetracantha Zone in which a renewed sea-level rise from neritic to more outer neritic conditions is inferred. All the while, oceanic influence and clear neritic input continues as well, especially at Eromanga-1 and Hughenden-7. These changes are less obvious in the more basinally located Manuka-1, where these conditions were already established in the previous zone and continued to prevail. In Hughenden-7 and Manuka-1 levels with a high influx of low salinity waters are apparent in the interval concerned. The interval is further characterized by a maximum in heterotrophic dinocysts, mainly consisting of *S. boydii*.

The transition from the *M. tetracantha* into the succeeding *C. denticulata* Zone represents a drop in sea level: in Hughenden-7 the outer neritic palaeoenvironmental dinocyst group (with influx of oceanic types) becomes virtually absent and in Eromanga-1 the dinocyst assemblages are very poor, while in Manuka-1 neritic and inner neritic influx is interpreted to become more important at the cost of oceanic influence.

Successively, at the onset of the *E. ludbrookiae* Zone, the renewed influx of minor oligotrophic elements indicates a temporary rise in sea level, which is followed by a sudden sea-level fall to littoral conditions. This sea-level fall is reflected in the middle of the Toolebuc Formation. The upper part of this unit and the remainder of the *E. ludbrookiae* Zone represent a gradual transgression to neritic conditions at Eromanga-1 and Manuka-1. The level in the middle Toolebuc Formation is associated with a strong increase in the heterotrophic dinocyst type *D. pusillum*.

Interpretation of the sporomorph records

The quantitative distribution patterns of the selected palaeoenvironmental sporomorph groups for Hughenden-7 (Figure 6), Manuka-1 (Figure 8), and Eromanga-1 (Figure 10) show that cool coastal and warm lowland vegetation prevailed over most of the studied intervals.

In Eromanga-1, the most southern located core, the distribution patterns show roughly four successive changes. Going from the ?*M. australis* into the *O. operculata* Zone, the lowland vegetation changes from wet and humid to drier circumstances. These drier conditions prevail over the succeeding *D. davidii*, *M. tetracantha*, and *C. denticulata* zones. While these conditions continue in the lower *E. ludbrookiae* Zone as well, a profound change toward cool and dry coastal vegetation occurs in the middle of the Toolebuc Formation. This vegetational change is of short duration because it shows a sudden return to the previous warm and dry lowland vegetation immediately after deposition of the Toolebuc Formation.

The extension of warm/dry coastal vegetation seems to change only slightly and shows no real apparent tendencies. The same accounts for the upland vegetation. River influence is constantly present, and shows only a minor extension in the *O. operculata* Zone.

The changes within the vegetation in Eromanga-1 can to a large extent also be observed in Manuka-1. However, the studied interval at Manuka-1 incepts at a slightly higher stratigraphical level than Eromanga-1 and the change within the lowland vegetation prior to the *O. opeculata* Zone cannot be observed.

One of the differences between the two records can be seen in the coastal warm/dry vegetation, which is hardly represented in Manuka-1. A further dissimilarity lies in the Toolebuc Formation; in Manuka-1 a subdivision within this unit is apparent but the coastal cool and dry vegetation, although showing an increase, does not show the high values as in Eromanga-1.

The record for Hughenden-7 shows the changes within the vegetation most detailed and the patterns seem cyclic in nature. The dominance of the cool and dry coastal vegetation alternates with that of the combined warm lowland vegetation. The latter vegetation dominates in the *O. operculata* Zone but a gradual change toward the cool and dry coastal vegetation is obvious. The warm lowland vegetation culminates in the middle of the *D. davidii* Zone from which point the reverse pattern occurs again to successively reach its nadir in he middle *M. tetracantha* Zone. At this level starts a second cycle, which ends just above the base of the *E. ludbrookiae* Zone.

While the cool and dry coastal vegetation for Eromanga-1 and Manuka-1 shows a strong increase within the Toolebuc Formation, a different pattern for Hughenden-7 emerges. Here this vegetation

type shows an increase from the start of the *E. ludbrookiae* Zone and prior to the Toolebuc, while the lowland vegetation diminished over the same interval to almost total absence.

5.3 *Integration of data for the three studied cores*

In this section relevant stratigraphical data is presented for the three studied cores in relation to the recognized dinocyst zones. The three cores are dealt with separately and the zones are discussed in ascending order.

5.3.1 *GSQ Hughenden-7*

O. operculata Zone: 151.18–177.00 m (larger part of isotope segment C8; Early Aptian).

The dinocyst palaeoenvironmental distribution patterns indicate an incursion of cool temperate oceanic and outer neritic waters, which is associated with low productivity conditions at the beginning of marine deposition. In this zone the the lowland vegetation reaches its maximum extension, whereas the coastal warm and dry vegetation, after having a maximum near the base, becomes virtually absent at the top of this interval. The whole interval corresponds to the major part of the *C. hughesii* Zone as differentiated by Burger (1982). The *O. operculata* zone represents the period of fastest rise in sea level and the consequent maximum flooding.

D. davidii Zone: 86.10–151.18 m (upper part of isotope segment C8, entire C9 and C10; Early Aptian).

The top of this zone is defined by the LO of *D. davidii*, in this case at 86.10 m. Burger (1982) already stressed that defining the zonal boundary is difficult because this level lies within a silty mudstone with traces of burrowing, infilling and crossbedding (from 80–100 m) and corresponds to a maximum influx of low salinity waters. Due to the character of the sediments it is considered that the actual LO of *D. davidii* could lie somewhat deeper within the core.

Burger (1982) suggested that the interval between 110 and 122 m corresponds to the Jones Valley Member. The upper boundary would also form the base of the *C. striatus* Zone (Burger, 1982). According to Morgan (1980b) the boundary between the Ranmoor and Jones Valley members correlates to the zonal boundary between his *E. turneri* A and B zones (equivalent of the boundary between the *D. davidii* and *M. tetracantha* zones in Helby et al., 1987), and the Jones Valley would lie in the upper part of subzone A (is the *D. davidii* Zone), as is the case in this study. Within this zone two further intervals with sandstones occur: 137–146 m and 148–150 m. These beds are considered quick shallowing episodes.

The early phase of sea-level fall is marked by an increase of heterotrophic elements (*D. davidii*) and a strong decease in cool temperate, outer neritic waters with a high oceanic influx. On the adjacent land, the cool coastal vegetation shows an initial extension but it diminishes again toward the top of this zone.
The zone contains benthic foraminifera characteristic of the *A. pitmani* Zone (Campbell and Haig, 1999).

M. tetracantha Zone: 68–86.10 m (isotope segment C11; Early Albian).

The relative cool temperate, outer neritic waters with increasing oceanic influx indicate a rise in sea level. An ultimate pulse of low salinity influx occurs above the burrowed and crossbedded, silty mudstone (80–100 m) and prior to a peak in heterotrophic elements (mainly *S. boydii*). This peak indicating enhanced productivity resulted in a minor increase in TOC. The transgression invoked several changes within the marine and terrestrial setting around Hughenden-7. It seems accompanied by: the appearance of planktic foraminifera, though still rare at 86.83 m

they become abundant and consistent above 64 m (immediately above the sandstone unit from 64-68m, at the base of the succeeding *C. denticulata* Zone); radiolaria, which are most persistent above 68 m (Campbell and Haig, 1999); and a strong reduction of upland vegetation.

In the present study the LO of *M. tetracantha* (used to define the top of the eponymous zone in Helby et al., 1987) occurs at 66 m. This agrees with the depth Burger (1982) inferred as top of the *M. tetracantha* Zone (as boundary between his *E. turneri* subzone B and C). However, a deviating position for the top of the *M. tetracantha* Zone has been chosen in this study, i.e., the top is put at 68 m (below the sandstone unit from 64–68 m) because this level marks profound changes in marine and terrestrial conditions in Hughenden-7. Therefore, the specimen of *M. tetracantha* at 66 m are considered reworked.

C. denticulata Zone: 37.29–68 m (isotope segment C12 and C13; Middle Albian).

Based on dinocyst palaeoenvironmental groups a sudden change to littoral conditions accompanied by an increase in low salinity waters is apparent in this zone; it indicates a sudden shallowing of the depositional environment. However, these changes are not reflected in other fossil groups or lithology: foraminifera, radiolaria and nannoconid fossils do not seem to be distinctly affected over the interval (see e.g., Campbell and Haig, 1999) and no lithologic change is referred to within the deposition of mudstones (Balfe, 1979).

E. ludbrookiae Zone: from 37.29 m upward (isotope segment C14 and C15; Late Albian).

This zone reflects warm marine and terrestrial conditions prior to deposition of calcareous shale and limestone of the Toolebuc Formation. The increase in the cool temperate coastal vegetation from the base upward indicates that these conditions are gradually changing. Changes in bathymetry are also apparent and from the base of the zone toward the Toolebuc Formation waters become increasingly neritic. This is accompanied by low salinity and littoral influxes, with outer neritic and oceanic incursions to a lesser extent as well. Within the Toolebuc Formation heterotrophic elements culminate (*D. pusillum*) while the coastal vegetation reaches ultimate expansion. The Toolebuc is further characterized by the presence of dwarf *Hedbergella* (planktic foraminifera) and the lack of bentic foraminifera (Campbell and Haig, 1999). The base of the *P. pannosus* sporomorph Zone lies at 28.50m (Burger, 1980), which agrees with the position within the lower part of the *E. ludbrookiae* Zone in the Helby et al. (1987) zonation scheme.
The base of this zone represents an initial fall of sea level, which is followed by a short-term rise and consecutive fall, before rapid transgression from the onset of the Toolebuc Formation.

5.3.2 *GSQ Manuka-1*

From the base of the studied interval to 741.11 m (latest Barremian?/earliest Aptian)

The lack of marine dinocysts probably indicates a fluvial setting with relatively cool vegetational elements dominating the coast in contrast to warm lowland vegetation.

O. operculata Zone: 658.07 – 741.11 m (isotope segment C7 and C8, Early Aptian).

This zone represents the incursion of cool temperate oceanic and outer neritic waters, associated with low productivity conditions at the beginning. During the zone the maximum extension of the lowland vegetation is reached, with cool coastal and upland elements throughout.
According to Campbell and Haig (1999) the interval concerned comprises part of three benthic foraminiferal zones: the *T. cusmani* Zone (727–724 m), an unnamed zone (724–680 m), and the lower part of the *A. pitmani* Zone (680–658.07 m). Campbell and Haig (1999) did not report planktic foraminifera from this interval.
This dinocyst zone is inferred to represent the period of fastest rise in sea level and the consequent maximum flooding.

D. davidii Zone: 600.00-658.07 m (uppermost part of isotope segment C8, entire C9 and C10; Early Aptian).

The decrease in cool temperate, outer neritic and oceanic waters in the lower half of this zone indicates a fall in sea level. This fall is accompanied by a marked increase of heterotrophic elements (*D. davidii*), which reaches a maximum in the sandstone unit from 633–637 m.

The upper half of the zone represents a renewed deepening. Conditions return to outer neritic with a strong oceanic influence and increasing inner neritic influx. While the warm lowland vegetation, with an important degree of cool coastal elements, is most extensive during the phase of sea level fall, the upland vegetation seems to expand during the renewed transgression.

At the top of this zone the strong decrease of outer neritic and oceanic waters, coeval with an increase in inner neritic waters, indicates a following sea level fall. This fall is further marked by a sandstone bed at the top of this zone, from 592–605 m, and an important change in the benthic foraminiferal assemblages to shallower conditions (Campbell and Haig, 1999). The interval was suggested to represent the Jones Valley Member by Balfe (1978). Its position at the top of the *D. davidii* Zone agrees with his assumption.

M. tetracantha Zone: 556.48–600.00 m (isotope segment C11 and C12; Early Albian).

The increase of relative cool temperate, outer neritic waters with additional oceanic and neritic influx in this zone, indicates a sea-level rise. On the adjacent land the cool coastal vegetation is most extensive while the upland vegetation strongly diminishes and the warm and dry lowland group expands. An ultimate low-salinity incursion occurs just below a glaucony-rich, muddy sandstone (from approximately 572–576 m in Campbell and Haig, 1999) and prior to a minor increase in heterotrophic elements (mainly *S. boydii*).

C. denticulata Zone: 546.00-556.48 m (isotope segment C13; Middle Albian).

This zone comprises two sandier intervals than in the intervals immediately above and below. The cool temperate, outer neritic waters undergo continued neritic influence but the decrease in oceanic influx, combined with an increase in inner neritic waters, indicates a relative sea-level fall.

Within this zone only benthic foraminifera of the *E. crespinae* Zone have been reported (Campbell and Haig, 1999)

E. ludbrookiae Zone: from 546.00 m upward (isotope segment C14 and C15; Late Albian).

The start of this zone corresponds to the base of the Toolebuc Formation. In the lower half of the Toolebuc the progressive transition from littoral through to oceanic waters indicate a rising sea level. This transgression is accompanied by an ultimate influx of heterotrophic elements in the middle of the Toolebuc, maybe indicating regained bottom water transport from shallower areas. This maximum in heterotrophics correlates with a peak value in TOC. Over the same interval the warm and dry lowland vegetation decreases, mostly at the expense of the cool coastal and to a lesser extent the warm coastal vegetation.

Successively, in the middle of the Toolebuc Formation, the relative deeper setting abruptly ends, which is followed by a renewed slow but gradual increase from littoral to outer neritic waters possibly reflecting a second deepening. Coeval with the second rise in sea level is the expansion of the warm lowland vegetation, which is increasingly influenced by coastal vegetation.

This zone is further characterized by the presence of dwarf *Hedbergella* (planktic foraminifera) and the lack of benthic foraminifera (Campbell and Haig, 1999).

5.3.3 GSQ Eromanga-1

?M. australis Zone: from the base of the studied section to approximately 730 m.

In this interval no marine dinocysts were encountered. In lithology a change from siltstone with minor sandstone and mudstone to sandier deposits was reported by Almond (1983), indicating a sea-level fall. On the surrounding land the warm lowland vegetation dominates, with decreasing relative numbers of cool coastal elements.

O. operculata Zone: 663.87–731.30 m (isotope segment ?C4 – C7 and lower half of C8; Early Aptian).

The zone represents a period characterized by incursion of cool temperate outer neritic waters with a strong oceanic influence. This is accompanied by an initial increase in primary productivity (*P. cretaceum*). At the base of the zone warm and dry lowland vegetation reaches maximum extension, changing to more wet/humid towards the top; cool and warm coastal and upland elements are present throughout. This zone represents the period of fastest rise in sea level to the consequent maximum flooding.

D. davidii Zone: 608.22-663.87 m (uppermost part of isotope segment C8, entire C9 and C10; Early Aptian).

The decrease in cool temperate, outer neritic and oceanic waters in the early part of this zone indicates a fall in sea level. Successively a minor rise is expressed by the return of outer neritic and oceanic dinocyst types, which diminish again toward the top where they are replaced by (inner) neritic elements with a high influx of low salinity indicators. Because a sandstone unit in the middle Doncaster Member of the Wallumbilla Formation (Almond, 1983) correlates to the top of the *D. davidii* Zone it is probably a lateral equivalent of the Jones Valley Member of the Wallumbilla Formation in northern sections of the Eromanga Basin. The dinocyst assemblages in the sandstone unit are realtively poor in taxa.

Throughout the *D. davidii* Zone heterotrophic elements (dominantly *D. davidii*) are well represented and reach maximum values in the middle of the zone. On land a gradual expansion of the warm lowland vegetation is apparent with a coeval increase in cool coastal elements and decrease in upland influence. The lowland-river vegetation expands most quickly in the younger part of the zone.

The total zone reflects an initial fall, a successive rise, and succeeding sharp fall in sea level.

M. tetracantha Zone: 530.67-608.22 m (lower part of isotope segment C13, entire C11 and C12; Early Albian).

The gradual increase of outer neritic waters with the successive influence of littoral, to inner neritic to neritic elements, indicates a sea-level rise. This transgression is followed by a sudden fall as indicated by a shift toward littoral and inner neritic waters from approximately 543.6 m. This change in depositional regime coincides with the boundary between the Doncaster and Coreena members. In Eromanga-1 the base of the latter is characterized by siltstone and sandstone, which is bioturbated in part, from 543.6 to 530 m.

The peak in heterotrophic elements (mainly *S. boydii*) in the lower half of this zone, accompanied by the strong influence of (inner) neritic waters, probably indicates transport from shallower areas. The increase in littoral and low-salinity influx in the younger part of this zone, show that this was a continuing process.

On land the warm lowland vegetation, undergoing continued cool and warm coastal as well as upland influence, is most expansive. The lowland-river vegetation slightly diminishes throughout the zone.

C. denticulata Zone: 482.11–530.67 m (isotope segment C13; Middle Albian).

This zone contains mudstone and muddy siltstone from 494.8 to 530 m, succeeded by interlaminated and interbedded sandstone and siltstone from 494.7 to 473.4 m. Dinocyst analysis is inconclusive because there are only scant specimen present throughout this interval. The change in lithology and the lack of dinocysts could reflect a relative sea-level fall but the vegetation and the distribution on the adjacent land seems a continuation of the vegetational development from the *M. tetracantha* Zone below and does not seem to indicate a sea-level change.

E. ludbrookiae Zone: from 482.11 m upward (isotope segment C14 and C15; Late Albian).

At the base of this zone lies the Toolebuc Formation. Within the formation heterotrophic elements culminate (*D. pusillum*) while the coastal vegetation reaches ultimate expansion as well. These maxima correspond to a peak in TOC and to an intraformational conglomorate, possibly indicating that this formation represents separate phases of deposition. Interesting to note is that various studies on sequences from the Eromanga Basin document a lithological division somewhere within the Toolebuc Formation (e.g., see the various lithological reports by the former BMR or GSQ).
Going from the base of the Toolebuc Formation toward its top, the palaeoenvironmental dinocyst groups (with *D. pussilum* put at hundred percent) show a change from more outer neritic and oceanic waters toward neritic followed by oceanic influence again. This is thought to represent an initial sea-level rise, which is truncated by the intraformational conglomorate, indicating a fall. This in turn succeeded by a minor rise from the second half upward again. From the onset of the second transgression within this zone, the warm and dry lowland vegetation reestablishes itself.

5.4 *Sequence stratigraphy*

The established timeframe, based on the recognition of global and local dinocyst events for the Eromanga Basin, enables correlation of the studied sections to the sequence stratigraphic framework of Hardenbol et al. (1998) and Jacquin et al. (1998).
In this study the oldest sequence boundary recognized is Ap3 (earliest Aptian), which represents the base of Transgressive Subcycle T13 of Jacquin et al. (1998). During this subcycle a profound marine incursion is documented in the Eromanga Basin, with the first evidence of marine dinocysts. The dinocyst assemblages are characteristic of the *O operculata* Zone. In Eromanga-1 (at 730 m) and Manuka-1 (at 739 m) Ap3 is put at the base of the first major sandstone unit below the interval comprising organic-carbon-isotope segments C4-C7, i.e. within the Cadna-owie Formation. For Hughenden-7 Ap3 is put at the base of the conglomorate (at 193 m) constituting the Gilbert River Formation.

Sequence boundary Ap 3 in Eromanga-1 and Manuka-1 lies within the Cadna-owie Formation. The lithological development in the interval prior to Ap3 shows a change from finer siltstone, minor sandstone and mudstone (lower Cadna-owie interval) to overall coarser sandstone (Wyandra Sandstone Member). This interval in Eromanga-1 and Manuka-1 is interpreted to reflect Subcycle R12d of Jacquin et al. (1998), and the subcycle exclusively comprising a series of Highstand System Tracts, i.e. of 3rd order cycles Ba6, Ap1 and Ap2 (Barremian to lowermost Aptian; Jacquin et al., 1998). Possibly the three 3rd order cycles are contained within the Cadna-owie Formation and the contact with the underlying Hooray Sandstone is a good candidate for one of the sequence boundaries. In either case the Aptian Stage boundary is situated below the studied intervals here.

Following the Transgressive Subcycle T13 is Regressive Phase R13 of Jacquin et al. (1998), encompassing the three 3rd order cycles Ap4, Ap5, and Ap6, which are possibly contained in the *D. davidii* Zone. In Hughenden-7 (at 150 m) and in Manuka-1 (at 658 m) Ap4 is put at the base of a sandstone unit; in Eromanga-1 Ap4 is less conspicuously expressed in lithology and is

tentatively put at the increase in *D. davidii*, around 668 m, an interval with lenses and laminae of very fine-grained and glauconitic sandstone.

Above sequence boundary Ap4, the reduction of outer neritic waters and the increase of littoral elements indicate a sea-level fall. This regression is accompanied by the strong increase in *D. davidii*, which culminates just below a sandstone unit. The base of the sandstone is inferred to represent cycle Ap5. The position of sequence boundary Ap5 in Hughenden-7 is at 140.60 m, in Manuka-1 at 637 m and in Eromanga-1 at 638.10 m.

The base of the succeeding sandstone, inferred to correspond with the Jones Valley Member at the top of the *D. davidii* Zone (Morgan, 1980b; Campbell and Haig, 1999), is considered to represent sequence boundary Ap6. For Hughenden-7, Balfe (1979) tentatively assigned the Jones Valley Member to the interval from 64 to 68 m. However, this level falls within *M. tetracantha* and not in the *D. davidii* zone, the position as inferred by Morgan (1980b), and for Hughenden-7 the Jones Valley is considered to correlate with the lower sandstone unit at 111.6 m. In Manuka-1 the Jones Valley lies at 605 m (in Campbell and Haig, 1999, taken as the Doncaster-Ranmoor Member boundary), and in Eromanga-1 around 620 m (below an interval with low numbers of dinocysts). This level falls within the top of isotope segment C10. According to Bralower et al. (1999) segment C10 corresponds with uppermost Aptian, and the top of C10 with the Aptian-Albian boundary. Jacquin et al. (1998) placed Ap6 in the uppermost Aptian, just below the Stage boundary as well.

The interval from Ap4 to Ap6 in Hardenbol et al. (1998) shows a relative stable, 2nd order sea level. Although, the interval containing the sequence boundaries Ap4 to Ap6 inferred for the three Eromanga cores seems to represent a deepening of the depositional environment, this is thought to be due to subsidence of the Eromanga Basin.

The *M. tetracantha* Zone incepts immediately above the Jones Valley Member (= Ap6). Consequently, the Aptian-Albian boundary falls within the sandstone member, at base of the associated dinocyst zone. The Jones Valley Member is considered to represent the relative abrupt sea-level fall at the end of Regressive Subcycle R13. This cycle is immediately succeeded by outer neritic waters and oceanic elements incurring again, which is considered the onset of the 2nd order Transgressive Subcycle T14 (Jacquin et al., 1987), but sample density did not allow unequivocal assessment of the 3rd order cycles Al1, Al2 and Al3. Burger (1982) discussed the dispute over dating the Jones Valley Member. Namely, based on the presence of the *C. striatus* sporomorph Zone Morgan (1980a) assigned an Albian age, while Day (1969) suggested an Aptian age based on shelly fauna found in outcrop. This may be related to the relative sea-level low during the Al1 and Al2 cycles, which could have resulted in erosion and a degree of re-working, obscuring the precise position of the Aptian-Albian boundary. Not being able to pinpoint the positions of the first three Albian sequence boundaries, the succeeding relative sea-level fall, marked by an increase in *S. boydii* below a sandstone unit in the *M. tetracantha* Zone, is inferred to represent the 3rd order variation within the 2nd order Regressive Subcycle R14, which would correlate to sequence boundary Al4 (Jacquin et al., 1998). In this case, Al1, Al2 and Al3 would fall prior to the increase in *S. boydii*. In Hughenden-7 sequence boundary Al4 would correspond to the level above the mudstone from 80–100 m; in Manuka-1 to the base of the sandstone below the increase in *S. boydii* at about 575 m; and in Eromanga-1 just prior to 589.54 m.

If the inferred Al4 for the Eromanga cores is correct, it should be followed by the major sequence boundary Al5 (Jacquin et al., 1998), and such a level seems present in all the cores. The onset of the *S. boydii* peak is succeeded by an increase in outer neritic and oceanic waters representing a rapid short-term sea-level rise. This increase ends abruptly below a major sandstone unit, which corresponds to the top of the *M. tetracantha* Zone in all cores. This level is inferred to represent the 3rd order major sequence boundary of cycle Al5. In Hughenden-7, Al5 would normally be put at the base of the associated sandstone unit (in this case at 68 m) but the dinocyst assemblages indicate that cycle Al5 ends above this level, at 60 m. In Manuka-1 Al5 lies at about

558 m, and in Eromanga-1 at 543.6 m, marking the boundary between the Doncaster and Coreena members.

The maximum flooding surface between Al4 and Al5 marks the Lower-Middle Albian boundary (Jacquin et al., 1998). In the Eromanga cores this level has been put at the maximum abundance of the oceanic dinocyst groups in between Al4 and Al5, in Hughenden-7 at 63.4 m, in Manuka-1 at 566.15 m and in Eromanga-1 at 547.28 m.

Successively in the *C. denticulata* Zone in Manuka-1, outer neritic waters remain constant to suddenly diminish at 544 m. This in combination with a decrease in oceanic, concurrent with an increase in littoral and neritic influx, is inferred to represent the 3rd order cycle Al6 (Jacquin et al., 1998), with the sequence boundary put at 544 m. This level in Manuka-1 corresponds with the top of the C. *denticulata* Zone and the base of the Toolebuc Formation.

In Hughenden-7 recognition of Al6 is not as straightforward and the top of the *C. denticulata* Zone does not seem to correspond with a sequence boundary. The next level possibly representing a sequence boundary lies at 60.9 m, which marks the top of an interval showing a transition in the palynological assemblages representing littoral waters at the base to minor outer neritic waters with oceanic elements and strong littoral and neritic influx at the top.

In Eromanga-1, the *C. denticulata* Zone comprises an interval with strongly reduced dinocyst numbers in a predominant sandy interval. Within the zone there is a transition from extremely low numbers of dinocysts near the base to higher numbers toward the top. This change is considered to represent a relative sea-level rise. Immediately above the *C. denticulata* Zone, at the base of the succeeding *E. ludbrookiae* Zone, dinocyst numbers are low again, representing a sudden fall in sea level. The boundary between the two zones at 486 m is therefore taken to represent sequence boundary Al6.

Within the *E. ludbrookiae* Zone lies the Toolebuc Formation. The extreme dominance of the heterotrophic dinocyst *D. pusillum* in the middle of this formation amidst mudstones, coeval with a decrease in oceanic and outer neritic influence, probably indicates a short-term sea-level drop and is inferred to represent sequence boundary Al7 of Jacquin et al. (1998), which defines the Middle-Upper Albian boundary. However, fluctuations within the palynological assemblages from this zone in Hughenden-7 might indicate one, and possibly two, short-term sea-level variations, indicating further sequence boundaries at 24.96 m and 27 m. In this case the sequence boundary within the Toolebuc Formation would correspond with Al9 from Hardenbol et al. (1998) and Jacquin et al. (1998).

The Allaru Mudstone, correlating with the upper half of the *E. ludbrookiae* Zone, shows a gradual deepening from littoral to outer neritic waters. This sea-level rise is inferred to represent the Transgressive Phase T15 of Jacquin et al. (1998).

6. Discussion

In chapters 2 and 3 of this thesis a series of FOs and LOs was determined to occur in Australian sections which are of significance in global biostratigraphic correlation. In this respect only the inception of *T. tenuiceras* and *C. granulatum* (earliest Aptian, see chapters 2 and 3) appear to be useful events in the studied Eromanga cores (GSQ Hughenden-7, GSQ Eromanga-1, and GSQ Manuka-1). Additionally, the FO of *L. arundum* permist direct correlation to ammonite calibrated Tethyan and Boreal successions; in Europe this particular event approximates the Aptian-Albian boundary (Leereveld, 1995; Hart et al., 1996). Although in Australian sequences this event is reported to coincide with the base of the *M. tetracantha* Zone (Helby et al., 1987), in the Eromanga cores it is situated above a sandstone unit within the lower *M. tetracantha* Zone.

Biostratigraphic correlation of the dinocyst events (e.g. LO of *V. magna*, FO of *T. tenuiceras*, FO of *L. arundum*) from GSQ Hughenden-7, GSQ Eromanga-1, and GSQ Manuka-1, shows that the studied intervals correspond with Aptian to Albian. This assessment is confirmed by the
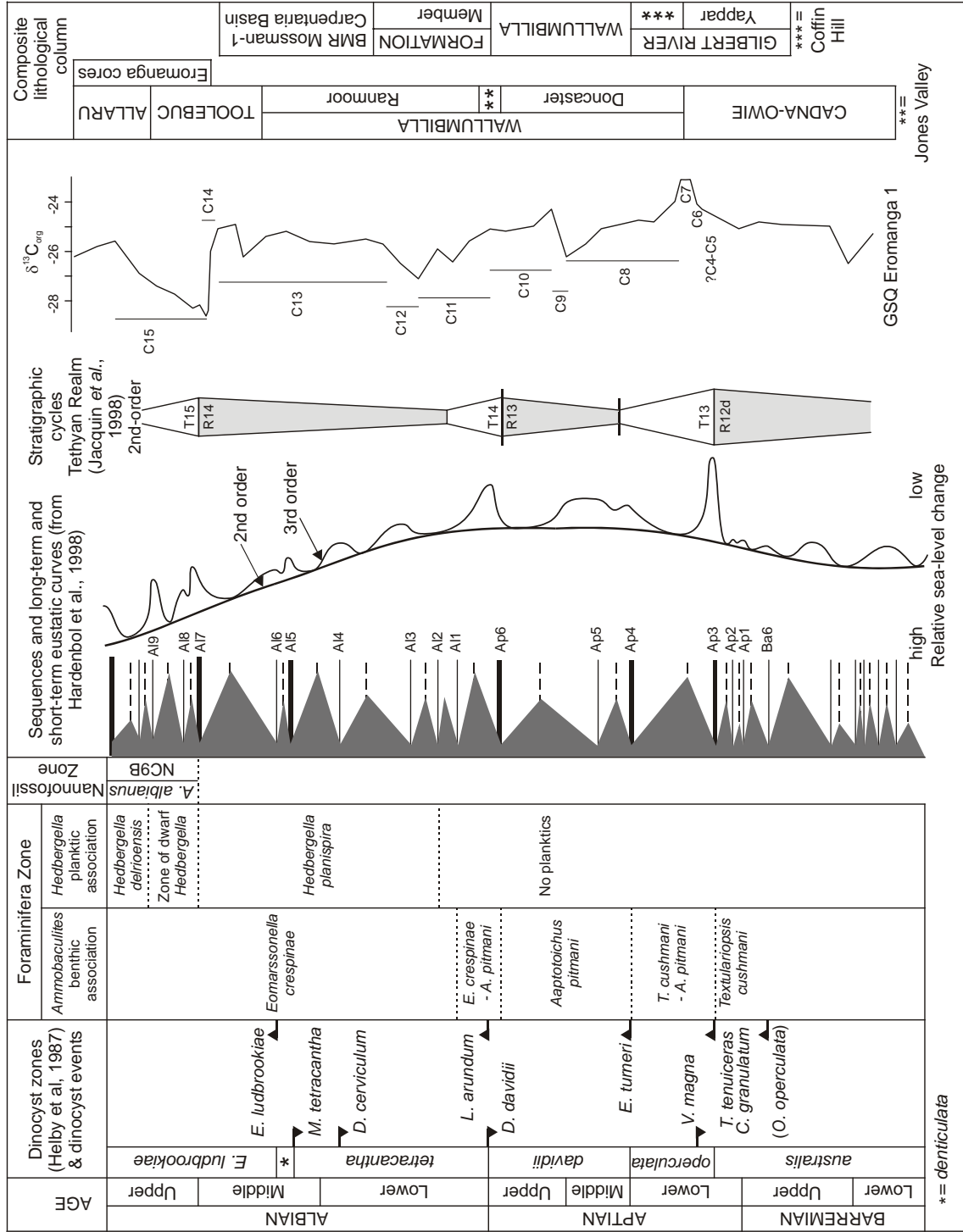
Extract from Morgan (1980a, figure 20), for full details see Figure 2.

SEA LEVEL CURVE

transgression

ε | δ | γ | β | α

AGE	FORMATION/Member
ALBIAN	HOORAY — WYANDRA / CADNA-OWIE
APTIAN	WALLUMBILLA — Yappar — Coffin Hill
	WALLUMBILLA — Doncaster — Ranmoor **
NEOCOMIAN	GILBERT RIVER

** = Jones Valley

Composite lithological column

*** = Coffin Hill

FORMATION	Member
WALLUMBILLA	Yappar ***
GILBERT RIVER	Carpentaria Basin
BMR Mossman-1	

Eromanga cores

ALLARU | TOOLEBUC | WALLUMBILLA (Ranmoor ** / Doncaster) | CADNA-OWIE

** = Jones Valley

$\delta^{13}C_{org}$ -24 -26 -28

C14, C15, C13, C12, C11, C10, C9, C8, ?C4+C5, C6, C7

GSQ Eromanga 1

Stratigraphic cycles Tethyan Realm (Jacquin et al., 1998) 2nd-order

T15 | R14 | T14 | R13 | T13 | R12d

Sequences and long-term and short-term eustatic curves (from Hardenbol et al., 1998)

2nd order
3rd order

low / high
Relative sea-level change

Al9, Al8, Al7, Al6, Al5, Al4, Al3, Al2, Al1, Ap6, Ap5, Ap4, Ap3, Ap2, Ap1, Ba6

Nannofossil Zone: NC9B — *A. albianus*

Foraminifera Zone

Hedbergella planktic association: *Hedbergella delrioensis*, Zone of dwarf *Hedbergella*, *Hedbergella planispira*, No planktics

Ammobaculites benthic association: *Eomarssonella crespinae*, *E. crespinae - A. pitmani*, *Aaptotoichus pitmani*, *T. cushmani - A. pitmani*, *Textulariopsis cushmani*

Dinocyst zones (Helby et al, 1987) & dinocyst events

E. ludbrookiae, *M. tetracantha*, *D. cerviculum*, *L. arundum*, *D. davidii*, *E. tumeri*, *V. magna*, *T. tenuiceras* / *C. granulatum*, (*O. operculata*)

Zones: *E. ludbrookiae* *, tetracantha, davidii, operculata, australis

* = denticulata

AGE	
ALBIAN	Upper / Middle / Lower
APTIAN	Upper / Middle / Lower
BARREMIAN	Upper / Lower

Figure 11. (Facing page) Composite correlation for the Eromanga Basin of dinoflagellate cyst zones (Helby et al., 1987) and events (this study); foraminifera zones (Campbell and Haig, 1999); nannofossil zone (Bralower et al., 1993); sequences, long and short-term sea-level variations (Hardenbolet al., 1998); stratigraphic cycles for the Tethyan Realm (Jacquin et al., 1998); $\delta^{13}C_{org}$ variations in GSQ Eromanga-1 from the Eromanga Basin (this study); generalized stratigraphic columns for the central Eromanga Basin and BMR Mossman-1 from the Carpentaria Basin; and comparison with the inferred sea-level curve and lithological correlation by Morgan (1980a) for the Eromanga and Carpentaria Basins.

recognition of the global carbon isotope segments C4 to C15, being characteristic of the Aptian - Upper Albian (see in Menegatti et al., 1998, and Bralower et al., 1999). Having the stratigraphical interval defined, the reconstructed sea-level fluctuations for the three Eromanga cores can be compared to the eustatic sea-level curve of Hardenbol et al. (1998) and Jacquin et al. (1998), allowing identification of the inferred cycles. It appears that most of the 2nd and 3rd order sea-level fluctuations can be recognized in the studied intervals, comprising 3rd order cycles Ap3 to Al7. The major sea-level changes were previously detected by, e.g., Morgan (1980a), Burger (1982), and Campbell and Haig (1999).

According to Morgan (1980b) and Burger (1982) boundaries of dinocyst zones seem to define boundaries of stratigraphical sequences. A relation is clear from the present study as well, but in general successive dinocyst zones incept above a sandstone units, instead of at the base. This indicates that the actual sequence boundary and the base of the related dinocyst zone are slightly offset.

In the lower part of the studied intervals from the Eromanga cores a same sequence of dinocyst events as in BMR Mossman-1 from the Carpentaria Basin (Chapter 3) can be observed, e.g. a peak in the heterotrophic dinocyst *P. cretaceum* combined with the global dinocyst events: LO of *V. magna*, FO of *O. operculata*, FO of *C. granulatum* and the presence of *T. tenuiceras*, correlating with global isotope segments C4-C6, which all occur just above sequence boundary Ap3. In Mossman-1 these events correlate to the uppermost Yappar Member of the Gilbert River Formation. In the Eromanga Basin, this interval lies at the top of the Cadna-owie Formation, inferring that it correlates to the Yappar instead of to the Coffin Hill Member as previously assessed (Morgan, 1980a; Figure 2 and 11). Additionally, Ap4 in Mossman-1 lies in the top of the *O. operculata* dinocyst Zone within the Coffin Hill Member (Chapter 3) and in the Eromanga cores in the upper *O. operculata* within the Wallumbilla Formation. Consequently, the Cadna-owie Formation is earliest Aptian in age instead of undifferentiated Neocomian (as indicated by Morgan, 1980a). The nature of the diachronism of sandstone formations between the Carpentaria and the Eromanga basins confirms observations made by Smart (1976), that the units in the Carpentaria Basin may be much younger than their equivalents to the south.

Morgan (1980b) proposed five transgressive phases of global sea-level fluctuations to be contained in the Cadna-owie to Allaru formations (Morgan, 1980b; Figure 2). He related the Cadna-owie Formation to a second transgressive phase in the basins. The Cadna-owie correlating to the upper Yappar Member instead of to the Coffin Hill Member, infers that the Cadna-owie correlates to the first transgressive phase. Consequently, the next lithological unit, the Wallumbilla formation, represents the second transgressive phase.

While the Yappar Member in the Carpentaria Basin represents a shallow marine, rather than fluviatile depositional environment (as presumed by Morgan, 1980b), it is time equivalent to non marine deposits contained in the Cadna-owie Formation from the Eromanga Basin. Prior to the extra fall of sea level of SB Ap3, in Regression Subcycle R12d (Jacquin et al., 1998), marine dinocysts are not represented in the studied facies from the Eromanga cores. The first incursion of dinocysts into the basin is related to the phase of rapidest sea-level rise of Transgression Subcycle T13 immediately following Ap3.

The successive lithological boundaries in the Eromanga Basin (from Cadna-owie to Wallumbilla, to Toolebuc, to Allaru) are considered progressive steps to more open marine facies. The transitions between the lithological units are inferred to fall within Transgressive Systems Tracts of cycles with varying duration, e.g., Ap 3 compared to Al5.

Based on foraminiferal data, Campbell and Haig (1999) defined four correlation intervals characterizing sea-level changes within the Eromanga Basin. After the initial transgression (within their correlation interval 1, above Ap3 in this study) a standstill in sea-level is reached. From this study this standstill is considered to correspond to the prolonged phase of maximum flooding of cycle Ap4 (Jacquin et al., 1998). The following initial shallowing at the beginning of their correlation interval 2 (Campbell and Haig, 1999) is inferred to corresponds with Ap5 in this study, the succeeding deepening episode with cycle Ap6, and the final shallowing at the top of this interval 2 with sequence boundary Ap6.

In the Jones Valley Member and its correlatives, the *M. tetracantha* dinocyst Zone incepts indicating that the Aptian-Albian boundary is contained within this interval, and consequently Al1 and Al2, and possibly Al3 as well. In Campbell and Haig (1999) the Aptian-Albian boundary lies within the benthic foraminifera *E. crespinae - A. pitmani* zones and just below the planktic *H. planispira* Zone. Based on the changes within the palynological assemblages and the inferred sequence boundaries for the Eromanga Basin, the planktic foraminifera (Campbell and Haig, 1999) seem to incept at the onset of the 2nd order Transgression Subcycle T14. Planktic forams were probably absent in the Aptian due to the low 2nd order sea-level of Subcycle R13, in combination with an extended period of 3rd order low (Hardenbol et al., 1998; Jacquin et al., 1998), leading to a shallow depositional environment; from Ap3 through to Ap6. At the onset of the Albian global sea level started to rise (2nd order T14, Jacquin et al., 1998; Hardenbol et al, 1998) and planktic foraminifera appear. According to Campbell and Haig (1999) a simultaneous change occurs in the restricted-marine benthic forams, which are replaced by normal salinity open-marine benthic foraminiferal faunas.

In many studied sequences Middle Albian deposits lie on top of Aptian deposits (e.g. Heilmann-Clausen and Thomsen, 1995; Menegatti et al.; 1998; Erba et al., 1999). Lower Albian is not represented due to a 3rd order sea-level low-stand leading and the succeeding deposits are Middle Albian and younger.

Correlation interval 3 of Campbell and Haig (1999), contains the inferred sequence boundaries Al4, Al5, and Al6, with the Lower-Middle Albian boundary within this interval. The Middle-Upper Albian boundary defined by sequence boundary Al7 (Jacquin et al., 1998), and correlating to the middle of the Toolebuc Formation, falls within correlation interval 4 of Campbell and Haig (1999).

The variations within the palynological assemblages, combined with the inferred global carbon isotope segments C14 and C15, allowed recognition of sequence boundary Al7 within the Toolebuc Formation. This implies that the Toolebuc event is correlative to OAE 1c and the associated organic rich shale equivalent to the Amadeus Segment in the Umbria Marche Basin (Italy). This age assignment is further supported by deductions made by Day (1969) and Bralower et al. (1993). According to Day (1969) the ammonites from the Toolebuc Formation are the first within this group which are similar to ammonites from outside the Eromanga Basin and of early Late Albian age. Bralower et al. (1999) studied nannofossils from the Eromanga Basin and combined with previous data from Shafik (1985) and foraminiferal data from Haig (1979), correlated the Toolebuc Formation with the *A. albianus* NC 9B nannofossil zone and the *H. infracretacea* foraminifera zone. These zones correlate to the UZA-2.1 sequence of Haq et al. (1988; Bralower et al., 1993), which comprises the early Late Albian sequence boundaries Al7 to Al9 of Hardenbol et al. (1998) and Jacquin et al. (1998).

The Toolebuc event, OAE 1c

During OAEs in the Early Cretaceous large amounts of organic matter were deposited over wide areas in different basins (Schlanger and Jenkyns, 1976; Jenkyns, 1980; Arthur et al., 1990). The deposition coincides with global rise of sea-level due to increased volume of ocean ridges (e.g. Larson, 1991). To explain the formation of organic rich deposits two different models are advocated, i.e., the preservation model (preservation is improved due to oxygen depletion by enhanced stratification of the water column (Schlanger and Jenkyns, 1976; De Boer, 1986), causing dysoxic or anoxic conditions at the seafloor due to enhanced stratification of the water column and resulting in better preservation of organic matter (e.g. Bralower and Thierstein, 1984), and the productivity model (enhanced primary productivity and higher consumption of oxygen during sedimentation of organic matter, eventually leading to a surplus, e.g., Pederson and Calvert, 1990; Erbacher et al., 1996; this model requires sufficient ventilation and nutrient recycling).

One of the Early Cretaceous OAE events is OAE 1c, which is contained in Albian sequences and has been recognized worldwide, e.g. from the Bay of Biscay (DSDP site 400), the Morocco Basin (DSDP site 370), the Naturaliste Plateau in the Indian Ocean (DSDP site 258), the Umbria Marche Basin (Italy), the U.S. Western Interior (Bralower et al., 1993) and from the Eromanga Basin (Australia). In all these sequences OAE 1c is characterized by peak TOC values and high $CaCO_3$ content. They further lack foraminifera or contain low diversity assemblages with no diagnostic markers (Bralower et al., 1993); from the Amadeus Segment (OAE 1c equivalent in the Umbria Marche Basin) Galeotti et al. (2003) reported small hedbergellids, similar to the observation made by Haig (1979) of dwarf *Hedbergella* within the Toolebuc Fm from the Eromanga Basin. Low diversity or opportunistic foraminifera taxa like *Hedbergella* are associated with increased primary productivity levels (Bralower et al., 1993; Galeotti et al., 2003). This would imply that the Toolebuc Fm was formed under the productivity model. Although, this is in agreement with previous assessments (e.g. Henderson, 1998, 2004) the palynological data from the present study shows that productivity levels were not uniformly high throughout the Toolebuc Fm.

Based on palynological, (micro)palaeontological and isotope stratigraphy a threefold subdivision within the Toolebuc Fm is apparent from the inferred sea-level variations, i.e. the lower Toolebuc reflects a 3rd order sea-level rise, followed in the middle Toolebuc by a sudden, short-term fall, and consecutive rise in the upper Toolebuc again. Seemingly different from previous studies where the whole of the Toolebuc was considered to relate to a regression as in Leckie et al. (2002) or to a transgression as in Henderson (2004). An obvious change within lithology also occurs, i.e. from dark gray calcareous shale with abundant laminae of crystalline calcite comprising bivalve remains of *Inoceramus* and *Aucellina* in the upper half, and dark, calcareous, pyritic shale with abundant fish remains in the lower half (Balfe , 1978, 1979; Almond, 1983).

The lower Toolebuc Fm shows diminishing $\delta^{13}C_{org}$ values and a coeval 3rd order transgression, confirming the assumption that variations within $\delta^{13}C$ reocords reflect sea-level variations (e.g. Gröcke et al., 1999). While such conditions are generally considered to represent periods of global warming, the lower Toolebuc reflects increasingly more cool-temperate and drier environmental conditions than in the adjacent intervals. Over the same interval primary productivity starts to increase and is parallelled by the TOC values. Interestingly, Campbell and Haig (1999) only encountered rare specimen of dwarf *Hedbergella* in samples which fall within the lower Toolebuc Fm, as inferred in the present study. Previously, the increase in productivity associated with the Toolebuc Fm was inferred to be caused by amplified volcanic activity along the eastern margin of the basin, and the subsequent nutrient flush by increased runoff (Henderson, 2004). However, this scenario contradicts the increasingly cool-temperate and dry conditions inferred for the lower half of the Toolebuc Fm, i.e. the palynological assemblages show no evidence of increased runoff during deposition of this part. Furthermore, Cook (1986) inferred that the organic matter from the Toolebuc Fm is mainly of marine origin contradicting increased

volcanism and associated high influx of terrigenous material for this part of the Toolebuc Fm. In the present study the relative sea-level rise in the lower part is considered to have caused leaching of nutrients on coastal plains and resulted in increased productivity in the adjacent basin due to which the oxygen minimum zone expands and a large portion of the formed organic matter preserved (e.g. Pederson and Calvert, 1990).

The level in the middle Toolebuc Fm representing a sudden, short-term sea-level fall correlates with the highest productivity levels reached for the Toolebuc. It further corresponds with maximum $CaCO_3$ content, maximum TOC values, and a minor positive shift in $\delta^{13}C_{org}$. From this interval Campbell and Haig (1999) reported abundant dwarf *Hedbergella*. This level corresponds to the characteristic gamma-ray peak for the Toolebuc Fm.

The positive correlation between enhanced productivity and high $CaCO_3$ content was documented from numerous micropalaeotological studies (e.g. Herbert et al., 1986; Premoli Silva et al., 1989; Erba, 1992; Galeotti, 1998, 2003) and the carbonate rich intervals are considered to have been deposited in relatively well mixed waters with good nutrient recycling (e.g. Galeotti et al., 2003).

The sudden sea-level fall probably caused a higher influx of detrital material, which has a lighter isotopic composition than marine organic material (e.g. Weissert, 1989) which in this case would result in more positive $\delta^{13}C_{org}$ values.

During the upper Toolebuc Fm, the $\delta^{13}C_{org}$ values and sea level both rise while the interpreted relatively more cool-temperate and drier conditions in the lower Toolebuc change to more wet and humid circumstances. These latter conditions could be related to increased volcanism as previously suggested. Whether this volcanism was of local character only (Henderson, 2004) is debatable since construction of the Central Kerguelen Plateau starts around this time as well (Larson and Erba, 1999; Leckie et al., 2002). And with the nature of the $\delta^{13}C_{org}$ records from the Eromanga Basin reflecting a global signature, it is suggested that it relates to the latter. Although, this does not exclude local volcanism taking place at the same time.

An increase in volcansim with the inferred warmer and wetter conditions for the upper part of the Toolebuc would cause an increase in terrestrially derived material. A higher influx of this isotopically lighter material into a marine setting would reflect as a positive shift in the $\delta^{13}C_{org}$ records, as can be observed for the Eromanga Basin. A higher influx would also result in increased primary productivity. However, based on palynology, in the upper Toolebuc Fm no further increase in primary productivity can be observed, instead heterotrophic dinocysts show a decrease. On the other hand, in samples from this interval studied by Campbell and Haig (1999) abundant dwarf *Hedbergella* occur, indicating increased primary productivity for the upper Toolebuc Fm.

Comparison of the three intervals within the Toolebuc Fm with the two models postulated for the formation of black shales in the Early Cretaceous all point toward the productivity model (e.g. Pederson and Calvert, 1990; Erbacher et al., 1996). However, the modes under which productivity increased is different for the three intervals, i.e., the lower interval relates to a rise in sea-level and nutrient leaching; the second to a sudden fall in sea-level and increased terrigenous influx; and the third to a sea-level rise, probably causing leaching of nutrients but also with a high input of terrigenous material. In further support of the productivity model is the presence of microplankton (e.g., dinocycts, nannofossils, foraminifera, radiolaria), ammonites, belemnites, and fish remains throughout, which indicate that the water column must have been oxygenated to some degree. Furthermore, the increase in $CaCO_3$ from the lower to the upper Toolebuc also indicates increase in productivity.

The reconstructed conditions for the Toolebuc from the present study are in agreement with the climatic changes inferred for the Early Cretaceous, i.e., the succession of events in the Toolebuc Fm shows a fluctuating pattern toward increasingly warmer environmental conditions.

Conclusions

Based on biostratigraphic correlation of dinoflagellate cyst events the investigated intervals from GSQ Hughenden-7, GSQ Eromanga-1, and GSQ Manuka-1, located in the Eromanga Basin, correspond with earliest Aptian to early Late Albian. This is confirmed by the synchroneity of the inferred sea-level signature for the Eromanga Basin and the eustatic sea-level curve of Hardenbol et al. (1998) and Jacquin et al. (1998) of which the 2nd and 3rd order regression-transgression fluctuations for the earliest Aptian to Late Albian could be identified (cycles Ap3 to Ap6 and Al4 to Al7). Additionally, all global isotope segments defined by Menegatti et al. (1998) and Bralower et al. (1999) for the earliest Aptian-Albian could be identified in the $\delta^{13}C_{org}$ curves for the three studied intervals from the Eromanga Basin.

Deposition of marine sediments in the basin started with the transgressive systems tract of the Ap3 sequence. Probably due to the shallow marine setting at this time no equivalent of a black shale related with OAE 1a was deposited and the global isotope segments C4-C6 are not well developed, but they do show the increase in $\delta^{13}C_{org}$ values prior to C7. The marine incursion at Ap3 is also characterized by cool-temperate waters and an increase in productivity, similar as in BMR Mossman-1 from the Carpentaria Basin for this time interval. Comparison of the succeeding organic-carbon-isotope stratigraphy from the three Eromanga cores with the Australian BMR Mossman-1 and with Tethyan and Boreal sequences revealed that the curves show identical changes. The boundary between the isotope segments C10 and C11, marking the Aptian-Albian Stage boundary, corresponds with the Jones Valley Member and approximates the base of the *M. tetracantha* Zone. The stage boundary marks the onset of the 2nd order transgressive systems tract T14.
Isotope segments C14 and C15 correlate to the Toolebuc Formation and represent a 3rd order sea-level rise, short-term fall (inferred to mark sequence boundary Al7) and consecutive rise again. This unit is associated with an increase in productivity, significant environmental change (relatively more cool-temperate and drier conditions during segment C14 in comparison to more humid and warm conditions during C15), and shows elevated TOC and carbonate levels. These characteristics and the comparison with the global stratigraphic scheme allows correlation of the Toolebuc with OAE 1c.

The bio- and chemostratigraphy in combination with the inferred sea-level fluctuations made refinement of the ages for the lithological units of the Eromanga Basin possible. The Cadna-owie Formation correlates to the Yappar Member in the Carpentaria Basin and is earliest Aptian in age, the lower Wallumbilla Formation from the Eromanga Basin correlates to the Coffin Hill Member from the Carpentaria Basin and is earliest Aptian. The Jones Valley Member of the Wallumbilla Formation marks the Aptian-Albian boundary, the remainder of the Wallumbilla Formation correlates to Early and Middle Albian. The Toolebuc Formation contains the Middle-Late Albian boundary, and the part of the Allaru Formation in the sections studied here is Late Albian.
The present study shows that the lithological boundaries represent progressive steps to more open marine facies, and are inferred to correspond to eustatic Transgressive Systems Tracts.

Within the lithological units from the Eromanga Basin five dinoflagellate zones, with a tentative sixth, from the Australian Mesozoic zonation scheme were recognized; in ascending order these are: *M. australis* Zone (tentative), *O. operculata* Zone, *D. davidii* Zone, *M. tetracantha* Zone, *C. denticulata* Zone, and *E. ludbrookiae* Zone.
The boundaries between the dinocyst zones coincide with sequence boundaries; the base of the *O. operculata* Zone corresponds with Ap3, *O. operculata* – *D. davidii* boundary with Ap4, D. davidii acme with Ap5, top *D. davidii* with Ap6, base *M. tetracantha* with top Jones Valley Member (inferred Al3), *M. tetracantha* – *C. denticulata* with Al5, and *C. denticulate* – *E. ludrbrookiae* with Al6. Consequently, the entire *O. operculata* and *D. davidii* Zone are Aptian, the boundary between

the *D. davidii* and *M. tetracantha* zones approximates the Aptian-Albian boundary, the *M. tetracantha* and *C. denticulate* zones are Early to Middle Albian, and the *E. ludbrookiae* Zone is Late Albian.

Composite dinoflagellate cyst species list for GSQ Hughenden-7, GSQ Manuka-1 and GSQ Eromanga-1

List of identified taxa

For documentation of the taxa identified in the present study, see the Lentin and Williams Index (Williams et al., 1998). A selection of taxa is illustrated in Plates 7 to 14 where sample codes, preparation slide numbers, size of the specimens and England Finder Co-ordinates (EFC) are indicated. For remarks on the encountered taxa is referred to the taxonomical sections in chapters 2 and 3.
The listed numbers refer to the order in the distribution data in Tables 7, 9, and 11.

	GSQ Hughenden-7 Table 7	GSQ Manuka-1 Table 9	GSQ Eromanga-1 Table 11	Plate 7	Plate 8	Plate 9	Plate 10	Plate 11	Plate 12	Plate 13	Plate 14
Achomosphaera spp		81	40								
Angustodinium acribes	60	44	62							a, b	
Aprobolocysta eilema			46							e, j	
Aprobolocysta sp.A (Stover & Helby, 1987)			48							c, d	
Aprobolocysta spp		45									
Apteodinium conjunctum			45								
Apteodinium granulatum	39	48	13						12f		
Apteodinium maculatum	15	9	24								
Apteodinium spp	61	63	91								
Ascodinium parvum		95								f	
Ascodinium spp			84								
Avellodinium lepidum	84	77	124								
Batiacasphaera spp	17	32	70								
Batioladinium spp	21	18	28							g-i	
Bourkidinium granulatum		75	79								
Callaiospaeridium asymmetricum	59	60	81								
Canningia spp	41	20									
Canninginopsis colliveri	16	13	16					11d-f			
Canninginopsis denticulata		94	108					11i, j			
Canninginopsis spp	54	52									
Cannosphaeropsis australis	73	86	104				10j-l				
Cannosphaeropsis peridictya	76	84	86				10g-i				
Cannosphaeropsis spp	56										
Cannosphaeropsis/Hapsocysta			49				10d, f				
Carpodinium granulatum		36	66						12g, h		
Cassiculosphaeridium pygmaea			71								

	GSQ Hughenden-7 Table 7	GSQ Manuka-1 Table 9	GSQ Eromanga-1 Table 11	Plate 7	Plate 8	Plate 9	Plate 10	Plate 11	Plate 12	Plate 13	Plate 14
Cassiculosphaeridium reticulata	30	24	63								
Cassiculosphaeridium spp	49	58									
Cernicysta helbyi		55								l, m	
Chlamydophorella solidus		43	43					11k			
Chlamydophorella spp		15						11m-q			
Circulodinium spp	35							11g, h			
Cleistosphaeridium spp	1	3	4								
Cometodinium spp	9	33	29								
Coronifera oceanica	11	12	22			9f					
Cribroperidiunium spp	8	7	18								
Cyclonephelium compactum			103		8a, b						
Cyclonephelium distinctum	28	11	2								
Cyclonephelium hystrix		97									
Cyclonephelium spp	29	78									
Dapsilidinium nyei	4	6	15								
Dapsilidinium spp	85	61	85								
Dapsilidinium warrenii	52		20								
Diconodinium davidii	45		75								14b-d
Diconodinium dispersum		59									
Diconodinium glabrum	64	96	97								
Diconodinium micropunctatum			30								14f, g
Diconodinium multispinum		91	106								
Diconodinium pusillum	48	66	68								14e
Diconodinium spp	40	46	82								
Dingodinium cerviculum	25	31	41								14j, m-o
Discorsia nanna	22	29	64			9e					
Druggidium deflandrei			72								
Druggidium rhabdoreticulatum	77		90								
Elytrocysta circulata			89								
Endoceratium exquisitum	71	74	100	7e, f, i							
Endoceratium ludbrookiae	83	89	109	7a-d							
Endoceratium polymorphum			94								
Endoceratium spp			80								
Endoceratium turneri	51	72	83	7g, h, j	8f, g						
Endoscrinium bessebae	7	16	7								
Endoscrinium campanula			50						12k		
Endoscrinium spp	78	79									
Epitricysta vinckensis			51							k	
Exochosphaeridium spp	38	37	19								
Fibradinium spp			96								
Florentinia deanei	70										
Florentinia khaldunii		62									
Florentinia mantellii	62		23								
Florentinia radiculata	58										
Florentinia spp	50	57	39			9a-d					

	GSQ Hughenden-7 Table 7	GSQ Manuka-1 Table 9	GSQ Eromanga-1 Table 11	Plate 7	Plate 8	Plate 9	Plate 10	Plate 11	Plate 12	Plate 13	Plate 14
Fromea amphora	31		31								
Fromea monilifera		40									
Fusiformacysta salasii			3								14a
Gagiella mutabilis	68										
Gonyaulacysta spp	12	34	25						12n		
Heslertonia heslertonensis	42	35	73								
Heslertonia spp	44	71									14r, s
Heterosphaeridium spp	86	70									
Hystrichodinium pulchrum	13	17	9								
Hystrichodinium spp	34	65	11								
Hystrichosphaeridium spp	65	21	44				10a				
Impagidinium spp	69	38	61								14p, q
Kallosphaeridium coninckii		19	21								
Kallosphaeridium spp	63										
Kiokansium polypes	53	30	69								
Kleithriasphaeridium eoinodes	74	56	32								
Kleithriasphaeridium spp			87								
Leptodinium hyalodermopsis			52						12i, j		
Leptodinium spp	19	23	76								
Litosphaeridium arundum	67	87	88			9g-l					
Litosphaeridium spp	79		99								
Meiourogonyaulax spp		41	67								
Microdinium alatum			98								
Microdinium spp		68	42								
Muderongia australis			53								
Muderongia crusis		69	54								
Muderongia mcwhaei		64	35		8h, j						
Muderongia spp	46	1	65								
Muderongia tetracantha	24	27	36		8e, i						
Nummus monoculatus	33	39	60							13n	
Odontochitina operculata	6	4	8		8c, d						
Odontochitina singhii	80	92			8k						
Odontochitina spp	72	93	101								
Odontochitina striatoperforata	75										
Oligosphaeridium pulcherrimum	20	83									
Oligosphaeridium spp	5	10	12								
Palaeoperidinium cretaceum	47	47	26								14h, i
Pareodinia ceratophora	23	26	37								
Pareodinia spp	37										
Pervosphaeridium spp	55	76									
Platicystidia eisenackii	36		47							13o	
Proloxisphaeridium conulum		90									
Proloxisphaeridium parvispinum	32	42	93								
Proloxisphaeridium spp	81		110								
Protoellipsodinium spinosum		85									

	GSQ Hughenden-7 Table 7	GSQ Manuka-1 Table 9	GSQ Eromanga-1 Table 11	Plate 7	Plate 8	Plate 9	Plate 10	Plate 11	Plate 12	Plate 13	Plate 14
Psaligonyaulax deflandrei			107						12l, m		
Pterodinium spp	87	88	33								
Rhabdoreticulatum spp			27								
Rhombodella natans	14	14	17							13p	
Sentusidinium aptiense		28	6								
Sentusidinium spp	2	2	1								
Spinidinium boydii	43	53	74								14k, l
Spinidinium spp	57	80									
Spiniferites spp	3	5	5								
Stephodinium spp		51									
Stiphrosphaeridium anthophorum		73	10				10b				
Systematophora areolata			55				10c				
Tanyosphaeridium spp	27	8	14								
Tehamadinium sousensis		50	78						12d, e		
Tehamadinium spp			105								
Tehamadinium tenuiceras		82	56						12a, b		
Tenua spp	66	67	34								
Trichodinium spp	18	22	59						12c		
Valensiella magna			57					11a, b			
Valensiella reticulata			58					11c			
Valensiella spp	82		92								
Wallodinium lunum	10	25	38							13q	
Yalkalpodium scutum	26	49	95							13r	

Plate 7

Light photomicrographs of key dinocyst taxa from the Eromanga Basin.

a, b, c, *Endoceratium ludbrookiae*, width central body 98 µm, Manuka-1 537.52m (2), EFC T26.
d, idem, width inner body 62 µm, Eromanga-1 460.73m (1), EFC H21.

e, f, *Endoceratium exquisitum*, width central body 101 µm, Manuka-1 610.00m (1), EFC X35/4.

g, h, *Endoceratium turneri*, width central body 90 µm, Manuka-1 528.10m (1), EFC J33/1.

i, *E. exquisitum*, width >98 µm, Eromanga-1 486.20m (1), EFC L48/4.

j, *E. turneri*, width inner body 80 µm, Eromanga-1 422.78m (1), EFC N25/3.

Plate 7
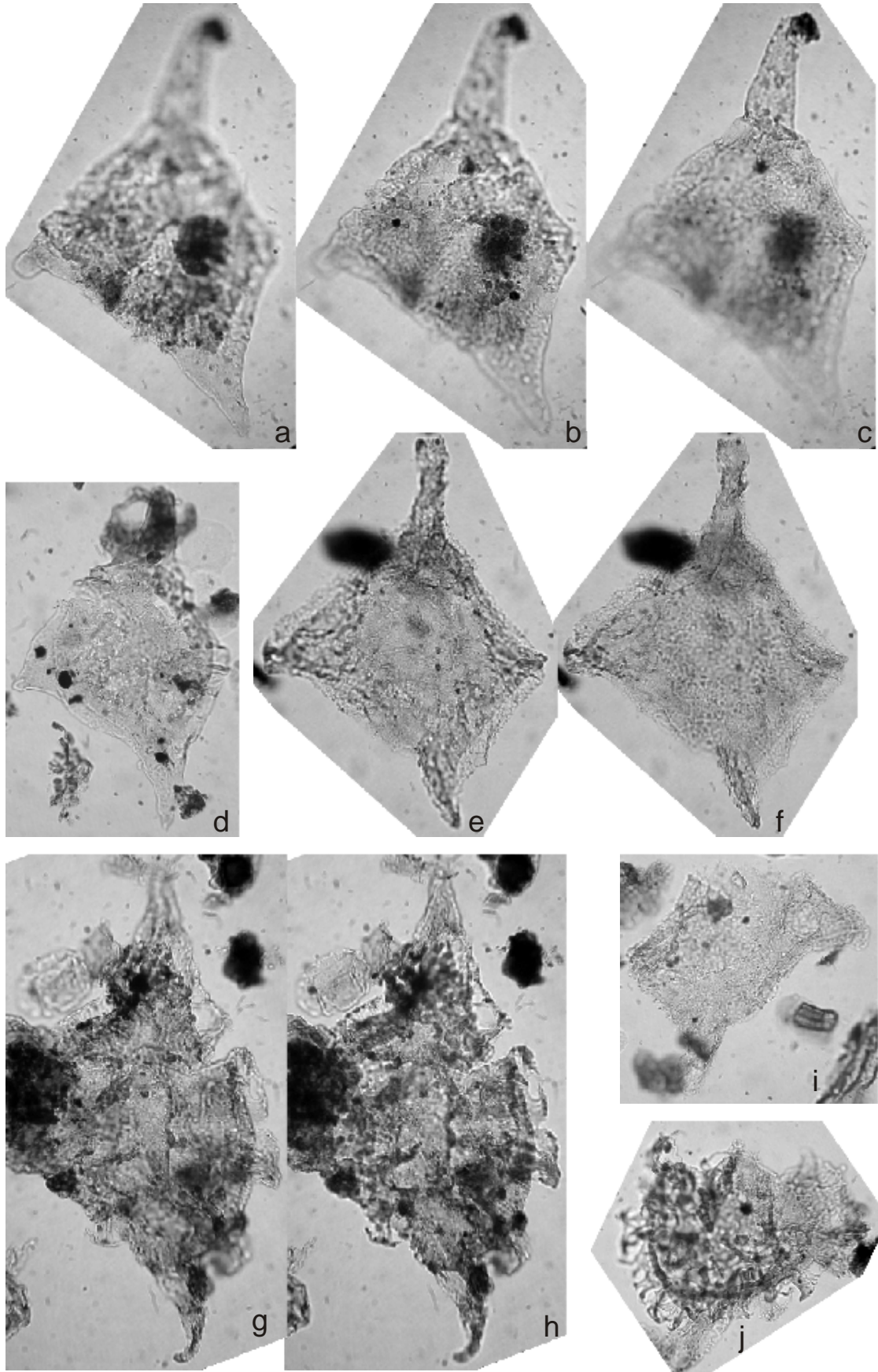
Plate 8

Light photomicrographs of key dinocyst taxa from the Eromanga Basin.

a, b, *Cyclonephelium compactum*, width 47 µm, Eromanga-1 443.25 m (1), EFC Q27/4.

c, *Odontochitina operculata*, width 65 µm, Manuka-1 704.52 m (1), EFC M20/1.
d, idem, width inner body 51 µm, Eromanga-1 715.83 m (1), EFC Q41/2.

e, *Muderongia tetracantha*, width inner body 50 µm, Eromanga-1 715.83 m (1), EFC Q42.

f, g, *Endoceratium turneri*, width central body 75 µm, Eromanga-1 572.75 m (1), EFC H27/3.

h, *Muderongia mcwhaei*, width inner body 92 µm, Eromanga-1 715.85 m (2), EFC R31/3.

i, *M. tetracantha*, body width 51 µm, Eromanga-1 638.10 m (1), EFC K52/1.

j, *M. mcwhaei*, width inner body 48 µm, Eromanga-1 715.83 m (1), EFC J36/1.

k, *Odontochitina singhii*, width 30 µm, Hughenden-7 60.90 m (2), EFC O32.

Plate 8
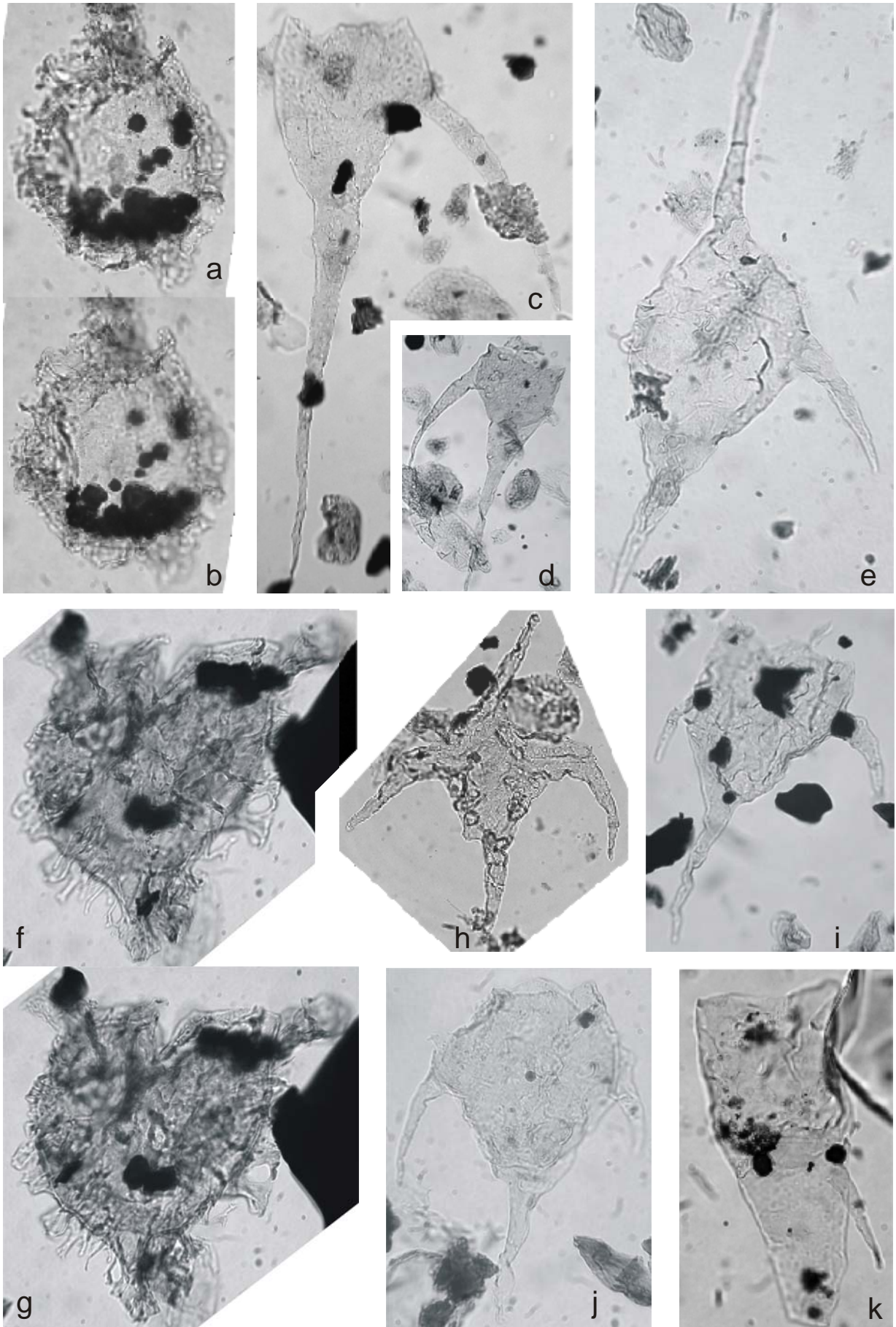
Plate 9

Light photomicrographs of key dinocyst taxa from the Eromanga Basin.

a, b, c, *Florentinia* spp , width inner body 44 μm, Eromanga-1 572.75 m (1), EFC R45.
d, idem, width central body 47 μm, Manuka-1 647.70 m (1), EFC L27.

e, *Discorsia nanna*, width inner body 26 μm, Eromanga-1 710.38 m (1), EFC Q31/1.

f, *Coronifera oceanica*, width central body ~33 μm, Eromanga-1 563.40m (1) EFC L55/3.

g, h, *Litosphaeridium arundum*, width central body 28 μm, Hughenden-7 76.00 m (2), EFC Q25/2.
i, idem, width central body ~25 μm, Eromanga-1 563.40 m (1), EFC M22/2.
j, k, idem, width central body 24 μm, Manuka-1 566.15 m (1), EFC J27/3.
l, idem, width central body 20 μm, Eromanga-1 471.44 m (1), EFC W34.

Plate 9
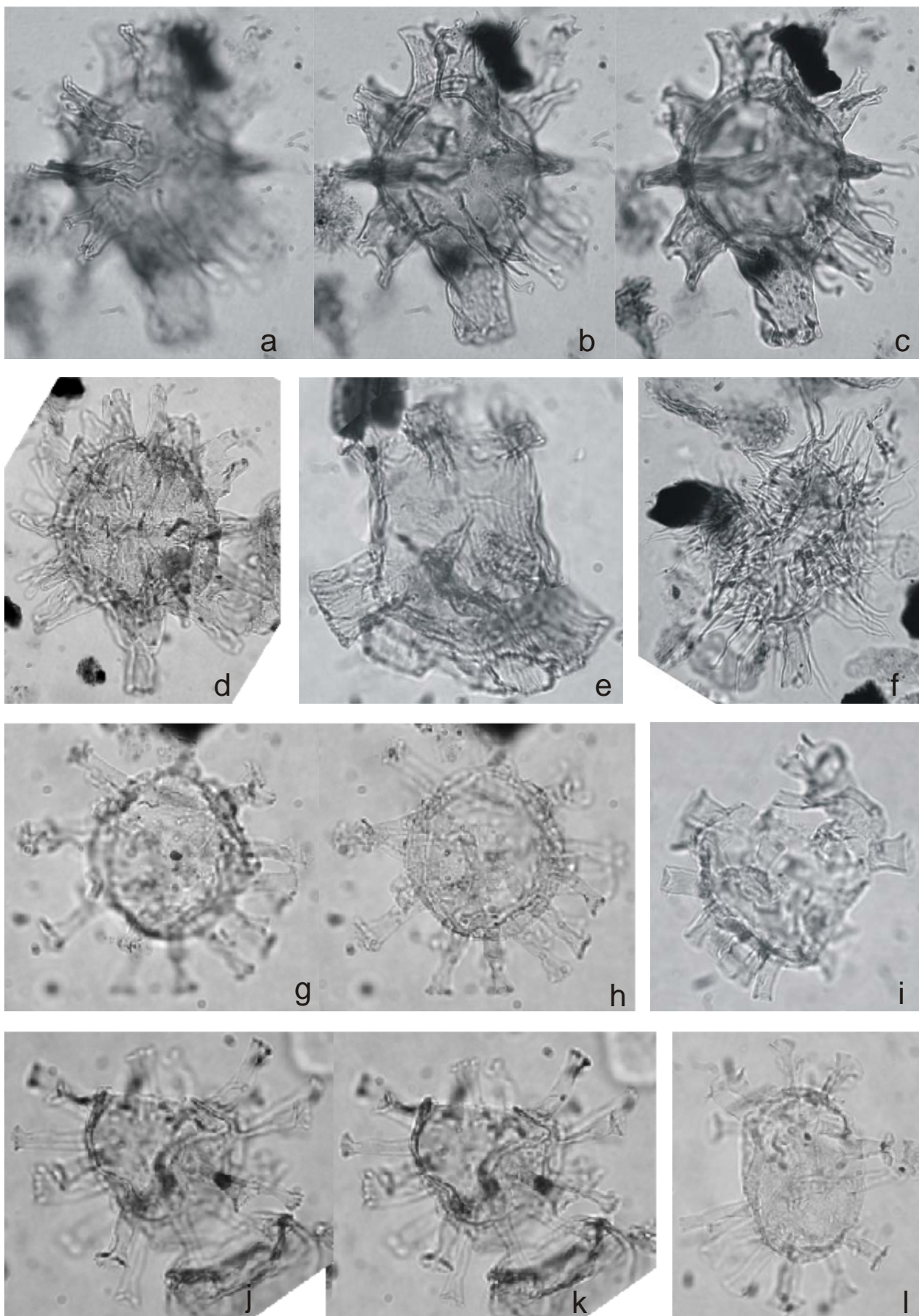
Plate 10

Light photomicrographs of key dinocyst taxa from the Eromanga Basin.

a, *Histrychosphaeridium* spp, width inner body 65 μm, Eromanga-1 715.83 m (1), EFC V45/2.

b, *Stiphrosphaeridium anthophorum*, width inner body 52 μm, Eromanga-1 715.83 m (1), EFC L27.

c, *Systematophora areolata*, width inner body 50 μm, Eromanga-1 715.83 m (2), EFC S38/2.

d, *Hapsocysta/Cannosphaeropsis*, width central body 42 μm, Eromanga-1 715.83 m (1), EFC F34.
e, f, idem, width central body 46 μm, Eromanga-1 715.83 m (1), EFC X41/3.

g, h, *Cannosphaeropsis peridictya*, max. length 64 μm, Manuka-1 579.18 m (1), EFC M37/4.
i, idem, max. length 83 μm, Manuka-1 566.15 m (1), EFC J30/1.

j, k, l, *C. australis*, width 52 μm, Hughenden-7 66.00 m (1), EFC T22/4.

Plate 10
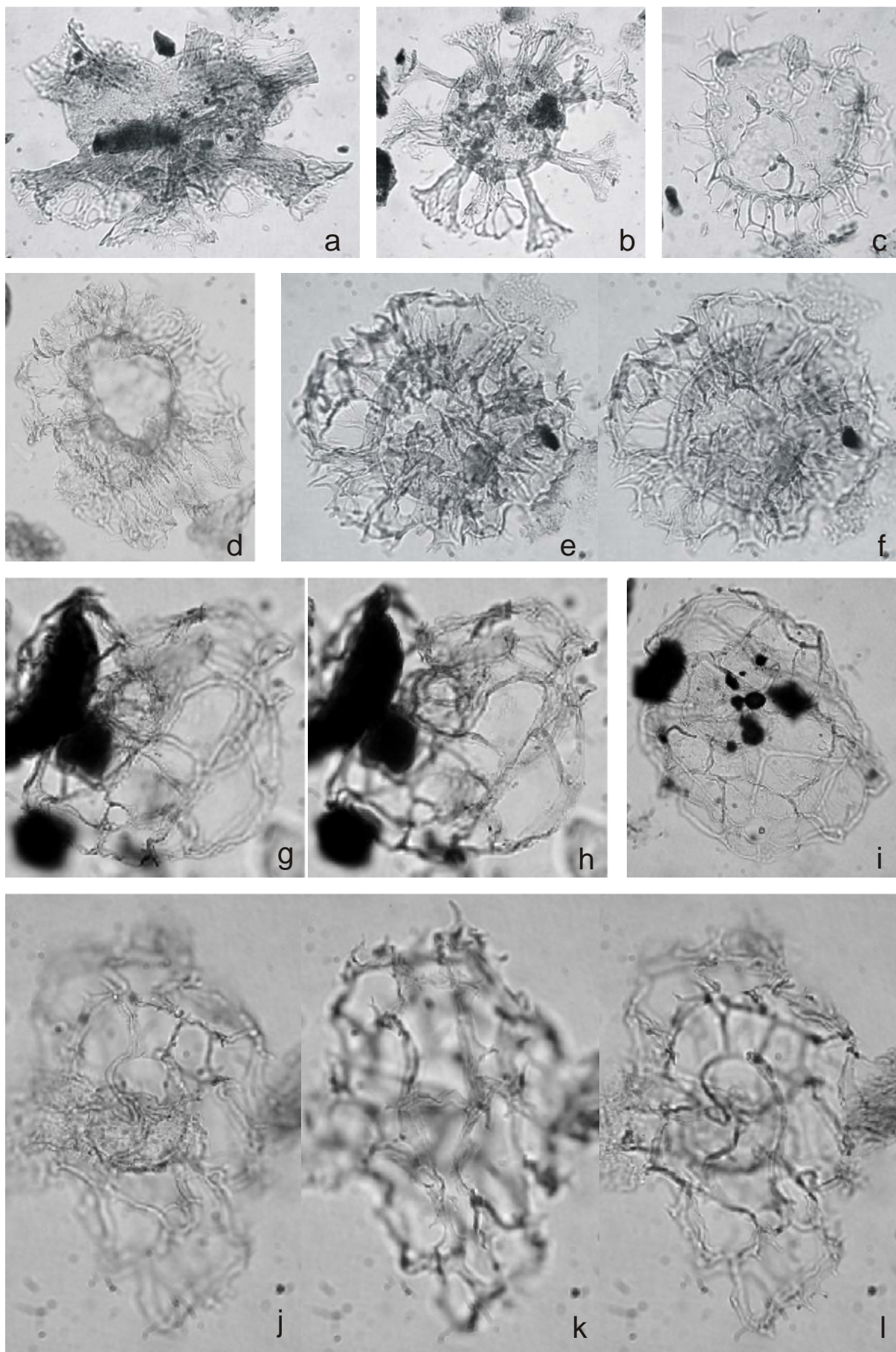
Plate 11

Light photomicrographs of key dinocyst taxa from the Eromanga Basin.

a, *Valensiella magna*, width 102 μm, Eromanga-1 715.83 m (1), EFC Y34/4.
b, idem, width 96 μm, Eromanga-1 715.83 m (1), EFC J45/2.

c, *V. reticulata*, width 40 μm, Eromanga-1 715.83 m (1), EFC K20.

d, *Canninginopsis colliveri*, width 66 μm, Eromanga-1 530.67 m (1), EFC H27/4.
e, idem, width 73 μm, Eromanga-1 530.67 m (1), EFC P26.
f, idem, width inner body 34 μm, Manuka-1 720.33 m (1), EFC N13/1.

g, *Circulodinium* spp, width 102 μm, Manuka-1 658.07 m (1), EFC V49/3.

h, *Cyclonephelium* spp, width ~75 μm, Eromanga-1 715.83 m (1), EFC J37/1.

i, j, *Canninginopsis denticulata*, width ~60 μm, Eromanga-1 401.86 m (1), EFC T29/4.

k, *Chlamydophorella solidus*, width 66 μm, Eromanga-1 715.83 m (1), EFC N36/3.

l, *Cyclonephelium-Canninginopsis*, width 84 μm, Eromanga-1 638.10 m (1), EFC S54/2.

m, n, *Dapsilidinium* spp, width central body 25 μm, Hughenden-7 76.00 m (2), EFC J44/3.
o, p, q, idem, width central body ~29 μm, Hughenden-7 151.18 m (1), EFC G12/3.

Plate 11
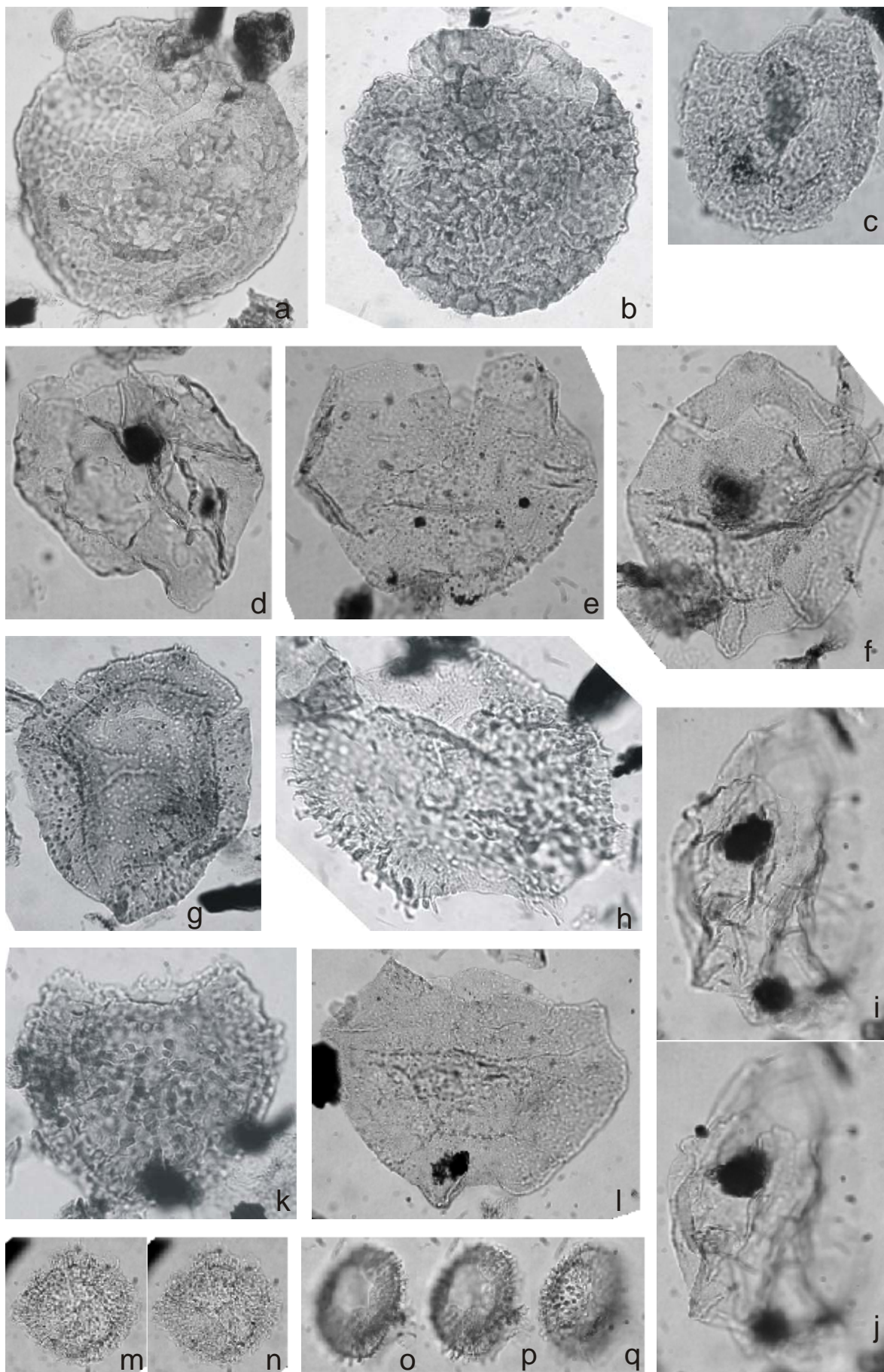
Plate 12

Light photomicrographs of key dinocyst taxa from the Eromanga Basin.

a,b, *Tehamadinium tenuiceras*, width 79 µm, Eromanga-1 715.83 m (2), EFC W41/3.

c, *Trichodinium* spp, width 57 µm, Eromanga-1 646.16 m (1), EFC R23/4.

d, e, *Tehamadinium sousensis*, width 57 µm, Eromanga-1 563.40 m (1), EFC U30.

f, *Apteodinium granulatum*, width 65 µm, Eromanga-1 422.78 m (1), EFC O24/2.

g, h, *Carpodinium granulatum*, width 28 µm, Eromanga-1 710.38 m (1), EFC L26/1.

i, *Leptodinium hyalodermopsis*, width 29 µm, Manuka-1 711.34 m (1), EFC L37/1.
j, idem, width 47 µm, Eromanga-1 715.83 m (1), EFC T34/4.

k, *Endoscrinium campanula*, width 45 µm, Eromanga-1 715.83 m (1), EFC M42/3.

l, m, *Psaligonyaulax deflandrei*, width inner body 45 µm, Eromanga-1 460.73 m (1), EFC O34/4.

n, *Gonyaulacysta* spp, width central body 42 µm, Eromanga-1 715.83 m (1), EFC H47/4.

Plate 12
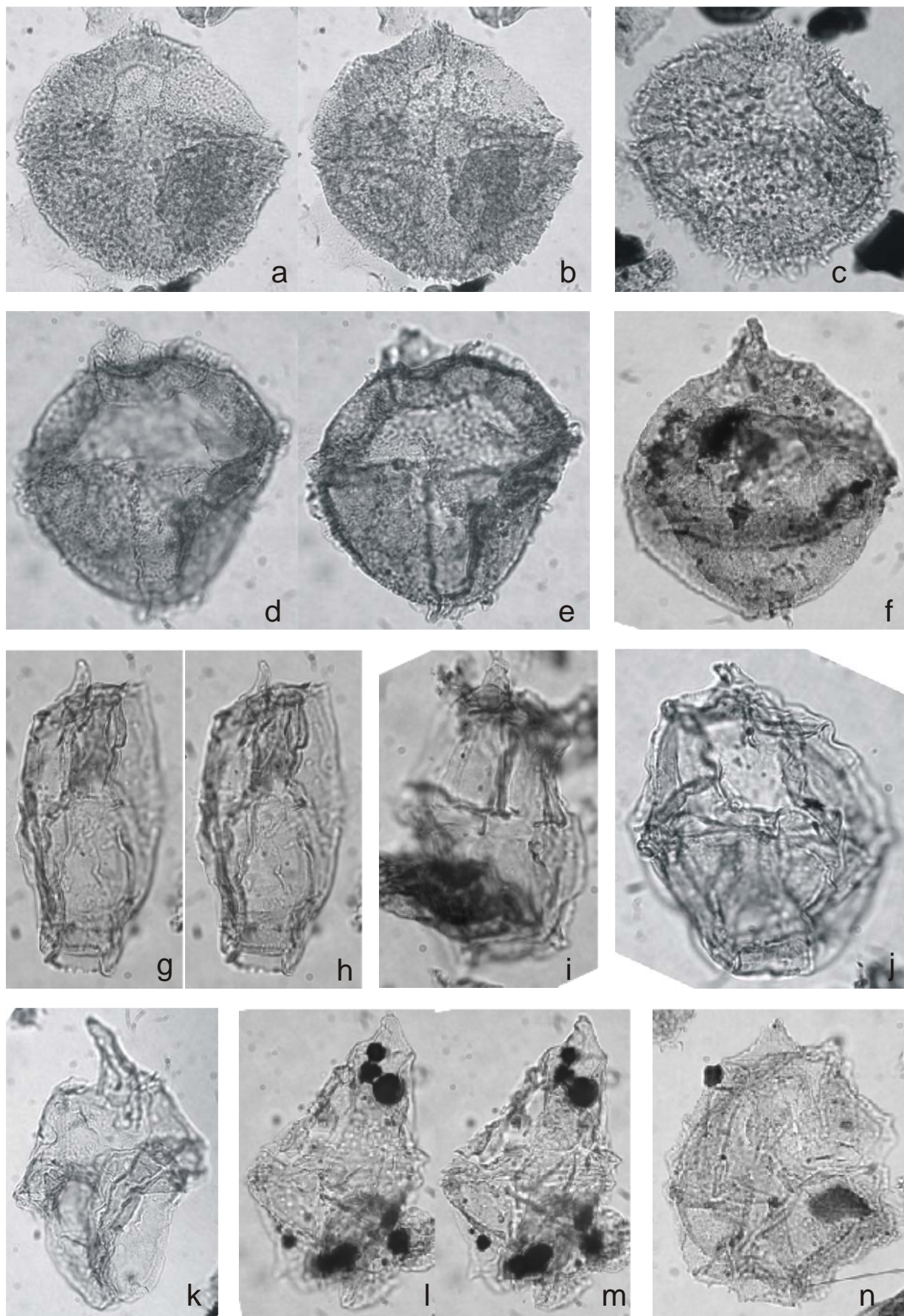
# Plate 13

Light photomicrographs of key dinocyst taxa from the Eromanga Basin.

a, b, *Angustodinium acribes*, width 17 μm, Manuka-1 681.82 m (1), EFC K45/3.

c, *Aprobolocysta* sp. A (Stover and Helby, 1987), width central body 37 μm, Eromanga-1 715.83 m (1), EFC J22.
d, idem, width central body 32 μm, Eromanga-1 715.83 m (1), EFC G30/3.

e, *A. eilema*, width central body 35 μm, Eromanga-1 715.83 m (1), EFC K25/3.

f, *Ascodinium parvum*, width central body 35 μm, Manuka-1 490.40 m (2), EFC H53.

g, *Batioladinium micropodum*, width 29 μm, Eromanga-1 715.83 m (1), EFC T39/2.

h, *B. jaegeri*, width 28 μm, Manuka-1 701.37 m (1), EFC L41.
i, idem, width 28 μm, Eromanga-1 715.83 m (1), EFC R29/2.

j, *Aprobolocysta eilema*, width central body 32 μm, Eromanga-1 715.83 m (1), EFC P49.

k, *Epitricysta vinckensis*, diameter ~50 μm, Eromanga-1 715.83 m (1), EFC Z31.

l, *Cernicysta helbyi*, width 41 μm, Manuka-1 701.37 m (1), EFC E12/4.
m, idem, width 34 μm, Manuka-1 658.07 m (1), EFC M28/3.

n, *Numus monoculatus*, width 35 μm, Eromanga-1 689.74 m (1), EFC G50/1.

o, *Platicystidia eisenackii*, width inner body 33 μm, Eromanga-1 715.83 m (1), EFC M21/3.

p, *Rhombodella natans*, width 36 μm, Eromanga-1 530.67 m (1), EFC L22/3.

q, *Wallodinium lunum*, width inner body ~25 μm, Eromanga-1 646.16 m (1), EFC A24/4.

r, *Yalkalpodium scutum*, width 88 μm, Manuka-1 658.07 m (1), EFC E38/1.

Plate 13

a

b

c

d

e

f

g

h

i

j

k

l

m

n

o

p

q

r
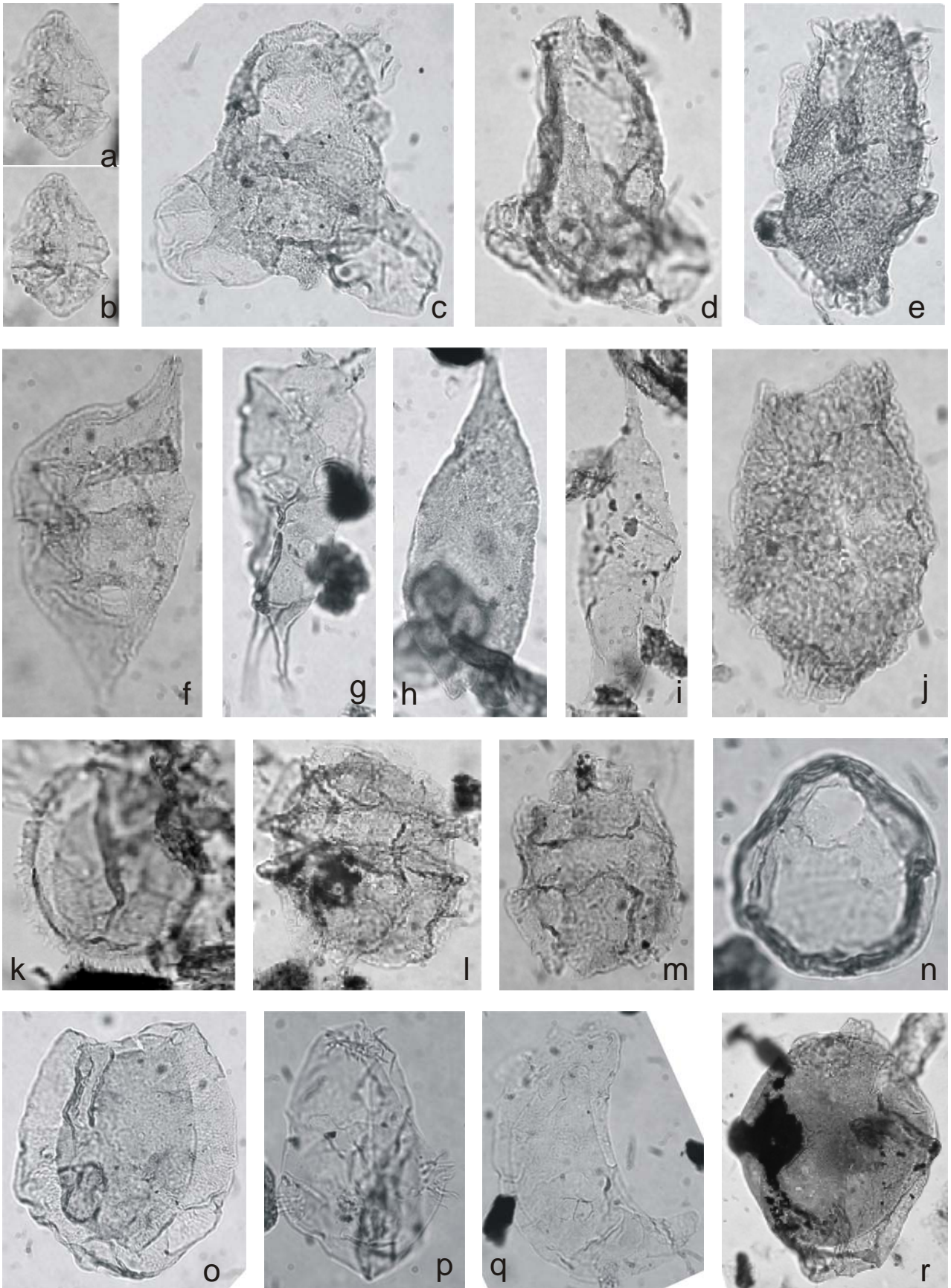
Plate 14

Light photomicrographs of key dinocyst taxa from the Eromanga Basin.

a, *Fusiformacysta salasii*, length 187 µm, Eromanga-1 785.00 m (1), EFC G36/2.

b, *Diconidinium davidii*, width 54 µm, Eromanga-1 646.16 m (1), EFC T22/2.
c, d, idem, width 46 µm, Hughenden-7 142.65 m (1), EFC M14/4.

e, *D. pusillum*, width 46 µm, Eromanga-1 422.78 m (1), EFC M47.

f, *D. micropunctatum*, width 32 µm, Eromanga-1 715.83 m (1), EFC S45/3.
g, idem, width 35 µm, Manuka-1 668.52 m (1), EFC K44/1.

h, *Palaeoperidinium cretaceum*, width 56 µm, Eromanga-1 715.83 m (1), EFC J22.
i, idem, width 58 µm, Eromanga-1 715.83 m (1), EFC H42/1.

j, o, *Dingodinium cerviculum*, width inner body 34 µm, Manuka-1 720.33 m (1), EFC N13/1.

k, *Spinidinium boydii*, width 36 µm, Eromanga-1 608.22 m (1), EFC G36.
l, idem, width ~40 µm, Hughenden-7 136.20 m (1), EFC H25/3.

m, n, *D. cerviculum*, width inner body 41 µm, Eromanga-1 715.83 m (2), EFC H19.

p, q, *Impagidinium* spp, width inner body 42 µm, Eromanga-1 689.74 m (1), EFC E46/4.

r, s, *Heslertonia* spp, width central body 48 µm, Manuka-1 546.00 m (1), EFC F30.

Plate 14